

Conjugated Polymers and Aromaticity

Miklos Kertesz,^{*,†} Cheol Ho Choi,[‡] and Shujiang Yang[†]

Department of Chemistry, Georgetown University, Washington, D.C. 20057-1227, and Department of Chemistry, Kyungpook National University, Taegu 702-701, South Korea

Received December 20, 2004

Contents

1. Introduction	3448
2. Conjugated Molecules and Simple Extended Systems	3452
2.1. Jahn–Teller (JT) Effects in Conjugated Molecules	3452
2.1.1. Cyclobutadiene, an Open Shell System	3452
2.1.2. Benzene, a Closed Shell System	3453
2.1.3. Pentalene and <i>s</i> -Indacene, a “Quasi” Open Shell System	3453
2.2. Peierls Distortions in Simple Extended Systems	3455
2.2.1. PA, a One-Dimensional Extended System	3455
2.2.2. Polyacene, a “Quasi” One-Dimensional Extended System	3457
2.2.3. Graphene, a Two-Dimensional Extended System	3458
2.2.4. SWCNs and Their Geometrical Properties	3458
2.3. Transition of Bond Alternation as a Function of Size: [14]- and [18]Annulenes, Closed Shell Systems with Low-Lying Excited States	3459
2.4. Alternation, Exchange, and Band Gap	3462
3. Conjugated Polymers	3465
3.1. PDA: A Prototype Conjugated Polymer with Two Nondegenerate Ground State Structures	3465
3.2. Ladder Polymers and Networks Built from Polyenes and PDAs	3468
3.3. Oligomer Size Dependencies of Conjugated Heteroaromatics	3469
3.4. Aromatic vs Quinonoid Structures of Conjugated Polymers	3471
3.5. Controlling the Band Gap of Conjugated Polymers through Change of Aromaticity	3474
4. Summary and Outlook	3476
5. Notations and Abbreviations	3476
6. Acknowledgments	3477
7. References	3477

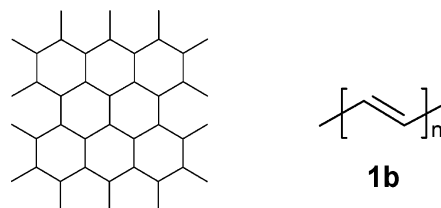
1. Introduction

Aromaticity is a useful concept in a variety of areas of chemistry including conjugated polymers, which is the focus of this review. Although loosely defined, the term “aromaticity”¹ was adopted originally to summarize the chemical behavior of a group of small organic compounds. Much of the current refinement of the concept of aromaticity is due to theoretical

chemistry as is well-reflected in the recent topical issue on the subject.² This review adds a further dimension to the discussion by looking at the consequences of the behavior of molecules at the very large size limit ($N \rightarrow \infty$, N is the number of π -electrons). Bond length alternation (BLA), defined as the difference between the long and short carbon–carbon bonds in a conjugated molecule,

$$\delta = R_{\text{long}} - R_{\text{short}} \quad (1)$$

has been considered as one of the phenomenological measures of aromaticity, with small or zero alternation indicating aromatic behavior and π -electron delocalization and larger alternation indicating π -electron localization and the absence of aromaticity.³ The second central theme of this review is another important property of large aromatic systems: their band gap. Bond alternation and band gap are two intimately connected properties of many large, extended conjugated systems. A sheet of graphite (graphene, **1a**) with all its CC bonds being equivalent is an ideal stable aromatic system in the large N limit with no alternation and zero band gap. Benzene has the same zero alternation but a substantial highest occupied molecular orbital (HOMO)–lowest unoccupied molecular orbital (LUMO) gap. *trans*-Polyacetylene (PA, **1b**), on the other hand, contains



1a

1b

somewhat localized alternating shorter and longer CC bonds. It has been recognized for a long time that the aromatic, antiaromatic molecules and acyclic polyenes display subtle variations in bond lengths.⁴ The concept of bond alternation can be extended from PA to other systems by using

$$\delta = \bar{R}_{\text{long}} - \bar{R}_{\text{short}} \quad (1')$$

where the bars indicate averages. (Note that in this article, we use δ to indicate actual or estimated values of the BLA, while the generalized coordinate along the alternation will be denoted by q ; see, e.g., eq 4.) Within Hückel theory, the highest occupied

[†] Georgetown University.

[‡] Kyungpook National University.



Born in Budapest, Hungary, Miklos Kertesz studied at the Eötvös Loránd University in his home town, under the guidance of Prof. János Ladik. Subsequently, he joined the research staff of the Central Research Institute for Chemistry of the Hungarian Academy of Sciences. After two postdoctoral years in the United States under the guidance of Prof. Hendrik Monkhorst and Prof. Roald Hoffmann, he joined the faculty of the Chemistry Department at Georgetown University in 1982. He was a Camille and Henry Dreyfus Teacher–Scholar in 1983–89. Prof. Kertesz has been visiting professor at the University of Vienna and the University of Nantes. His work focuses on understanding the structural, electronic, vibrational, and magnetic properties of molecules, polymers, and crystals on the basis of molecular orbital and crystal orbital calculations. His interests include designing new materials with desirable physical properties, conducting polymers, nanotubes, aromaticity, solid state chemistry, and intermolecular interactions in organic solids.

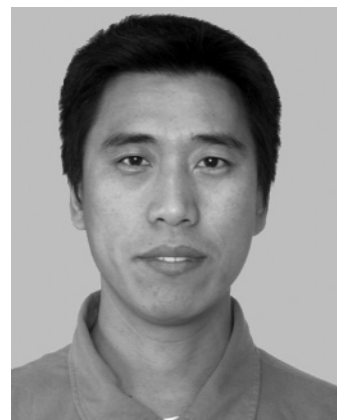


Cheol Ho Choi was born in Taegu, South Korea. He studied chemistry at Seoul National University, where he obtained his B.Sc. and M.Sc. degrees in 1990 and 1992. He carried out his doctoral studies under the guidance of Prof. Miklos Kertesz at Georgetown University, Washington, D.C., and was awarded his Ph.D. degree with Distinction in 1998. He worked with Prof. Mark S. Gordon as a postdoc at Iowa State University/Ameslab during 1998–2000. Since then, he has joined the chemistry faculty at Kyungpook National University in Taegu, South Korea. Prof. Choi's main research interests lie in the mechanistic understanding of interfacial chemical reactions, which include organic functionalization of semiconductor surfaces. He is also interested in the development of quantum theories for large systems and their applications to chemical systems.

orbital (HOO) to lowest unoccupied orbital (LUO) gap, E_g , of PA is proportional to the bond alternation:⁴

$$E_g = E_{\text{LUO}} - E_{\text{HOO}} = c_{\text{altern}} \cdot \delta \quad (2)$$

We use the subscripts LUO and HOO to refer to both molecular and crystal orbitals (COs), whichever is appropriate for molecules and polymers, as the case may be. This description of the energy band gap (E_g)



Shujiang Yang was born in 1971 in China. He received his B.S. degree in chemistry from Nankai University in 1993. He continued his graduate study in Nankai and obtained his M.S. degree in 1996 under the supervision of Prof. Lurang Pan, majoring in physical chemistry and subjecting in petrochemical catalysis. This led him to get a research position in Shanghai Research Institute of Petrochemical Technology, China Petrochemical Corporation (SINOPEC), after graduation. After 4 years of research work with SINOPEC, he came to the United States in 2000 to seek his Ph.D. degree in chemistry. He began his Ph.D. program in Prof. Lowell Kispert's research group at the University of Alabama studying the role of carotenoids in photosynthesis. A year later, he transferred to Georgetown University to start his Ph.D. program in theoretical chemistry under the guidance of Prof. Miklos Kertesz. His major research interests involve the quantum mechanical study of low band gap conjugated polymers and carbon nanotubes.

for a conjugated polymer establishes a deep connection between the bond alternation parameter and a fundamental electronic property, placing these two to the center of discussion in this review. The relationship between bond alternation and band gap is more complicated in the general case when heteroatoms, fused rings, and interchain links may obscure the central role that BLA plays in influencing properties. Section 3.4 is devoted to the related problem of the aromatic to quinonoid (AQ) valence tautomerization. Even in the prototypical case of PA, electron correlation effects complicate the relationship between the structural parameter of bond alternation and the electronic property of band gap. Generally, the correlation contribution to the band gap cannot be separated from the alternation contribution. For a limited type of calculation, a simplified expression has been derived that includes both the previous bond alternation term and an electron correlation term:⁵

$$E_g = [(c_{\text{altern}} \times \delta)^2 + (E_g^{\text{correl}})^2]^{0.5} \quad (3)$$

It is very important from the chemical point of view that heteroatomic substitutions, the presence of fused rings, cross-links, and other structural motifs strongly influence the band gap. These effects appear on top of the effect of the bond alternation and electron correlation, and the actual gap is a result of these various modifying components. These issues will be addressed in section 3.

Other indices of aromaticity that are primarily based on bond alternation have been suggested including the aromatic stability index,⁶ the harmonic oscillator model of aromatic stability (HOMAS),⁷ V

indices,⁸ harmonic oscillator stabilization energy (HOSE),⁹ and the theory of double-bond fixation in conjugated molecules.¹⁰ These other indicators have been amply reviewed in the present and previous topical issues of *Chemical Reviews* mentioned in ref 2. Connections between aromaticity indices are well-established.¹¹

In this review, we shall discuss the consequences of BLA and the HOMO–LUMO separation for smaller and very large aromatics. Furthermore, conjugated polymers, which exist in the large N regime, offer interesting problems in aromaticity, some of which we shall also address. Since the discovery of the remarkably high conductivity of doped PA,¹² π -electron conjugated polymers have attracted much interest. Since then, many π -conjugated polymers have been synthesized in the search for useful new materials. Discoveries of their novel properties such as nonlinear optics, electroluminescence, and photovoltaics are leading to device applications.¹³ A common theme in the literature is the design and synthesis of low band gap polymers with appreciable bandwidth.¹⁴ The sufficient bandwidth of at least a few tenths of an electronvolt is required to ensure sufficient mobility along the chain while the small gap is desirable for a variety of interests.^{13,14}

Theoretical understanding, especially via electronic structure theory, has helped substantially to formulate a microscopic conceptual framework within which the physical properties of these organic polymeric materials are being interpreted and analyzed. One of the fundamental parameters is the aforementioned BLA,¹⁵ which goes also by the name of the amplitude mode,¹⁶ ja-mode,¹⁷ or simply Peierls mode.¹⁸ The vibrational mode associated with this BLA, an antisymmetrical stretching mode, is strongly coupled with the electronic structure of conjugated polymers.¹⁹ This strong coupling is expressed in eqs 2 and 3 indicating the direct effect on E_g of the changing degree of alternation while the molecule vibrates along this vibrational mode.

Thus, bond alternation plays a key role in both conjugated molecules and extended systems. Qualitative discussions of relative stabilities of conjugated systems often invoke the concept of aromaticity.

Three common types of potential energy surfaces (PESs) along the valence tautomerization reaction coordinate

$$q = a\delta \quad (4)$$

are illustrated in Figure 1: part a represents one minimum at the “delocalized” form; part b has two minima at two equivalent “localized” forms; and part c has three minima with one at the “delocalized” and two more at the “localized” forms. Although the detailed shapes of the PESs vary from system to system, the basic trend should fall into one of these main categories. Note that parameter a connects the minima linearly, which may not be the proper reaction coordinate; thus, Figure 1 should be viewed as a qualitative illustration. As we shall see, various theoretical models indicate qualitatively different PESs. In general, the workhorse of quantum chemistry, the Hartree–Fock (HF) theory, clearly over-

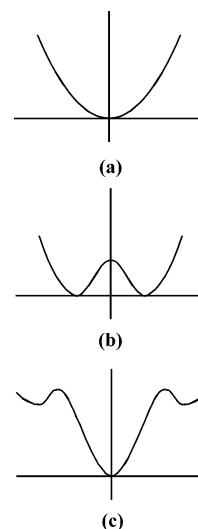


Figure 1. Illustrations of PESs along the BLA coordinate, q (see eq 4). Parts a–c correspond to one minimum at the delocalized form, two minima at two degenerate localized forms, and three minima, respectively.

estimates the degree of BLA; thus, the effects of electron correlation play an important role in helping to establish the correct energetics of the systems being described here.

This review begins with the similarities and differences of the nature of BLA in the two limiting small conjugated systems: antiaromatic cyclobutadiene and aromatic benzene. Then, we establish connections between conjugated polymers and conjugated molecules and eventually obtain a more general view of the electronic structure–geometry relationships as a function of molecular size. The geometry and electronic structure of conjugated polymers will be discussed in terms of the balance between aromatic and quinonoid structures in section 3.

A few comments on methodology are in order. As quantum chemistry has evolved, reliable techniques have become widely available. In this paper, we refer to a variety of methods that have been employed in the theoretical determination of structural, energetic, vibrational, and other characteristics of molecular and polymeric systems. Theoretical methods for the latter are less widely known. Coulson,²⁰ Longuet–Higgins and Salem (LHS),⁴ Koutecky and Zahradnik,²¹ Ladik and co-workers,²² Popov and Shustorovich,²³ Andre and co-workers,²⁴ and Whangbo and Hoffmann²⁵ were some of the pioneers who developed and applied quantum chemical techniques for polymeric molecules and the solid state. Recently, there has been a large increase in the use of solid state methods within the chemistry community, many borrowed from physicists and applied for crystals, polymers, surfaces, and films. A few molecular computer codes already have a solid state (often under the category of “periodic boundary conditions”, PBC) option,²⁶ and great many more computer codes are available for solid state calculations per se. A large portion of the solid state codes employ plane waves as the basis set, rather than atomic centered orbitals, but in nonempirical (ab initio) calculations, suf-

ficiently large basis sets should give essentially identical results independently from the basis set.²⁷ Several reviews are available,²⁸ which introduce the language of k -space, Brillouin zones (BZs), and energy bands necessary to discuss the electronic structures of extended systems, such as conjugated polymers, carbon nanotubes, and graphite.

The rest of this section is a brief summary of solid state concepts used in this review and may be skipped for readers familiar with k -space, BZs and energy bands, band gaps, and densities of states. Suppose that there is a large number (N) of identical repeat units, called a unit cell, in a macromolecule or some other extended system. Assume that there are m states within the unit cell. The mN states of the whole large system can be labeled by symmetry indices if there is perfect periodicity, an assumption that may be fulfilled exactly or approximately. Periodicity implies that translation, R , is a valid symmetry operation: $R = l_1a_1 + l_2a_2 + l_3a_3$ (a_1 , a_2 , and a_3 are the lattice vectors, and the three l s are integers). In one dimension, there is only one a vector; in two dimensions, there are two. This symmetry allows the use of " k " symmetry labels, which can be arranged as k -vectors in a k -space (reciprocal space) that has the same dimension as the system being studied. k -space is also periodic; the most symmetrically chosen unit cell in k -space is called the Brillouin zone. Points in k -space can be expressed as $k = k_1b_1 + k_2b_2 + k_3b_3$. A straightforward interpretation is that the phases of wavefunctions separated by a lattice vector R at any k -point are equal to $\exp(ikR)$. For example, the phase for any translation is 1 at the $k = 0$ special point (Γ -point). (For the arcane notation of BZ special points, see ref 29.) The number of states in the BZ is N , so to each k -point in the BZ there correspond m states, yielding the total of mN states. In the $N \rightarrow$ infinity limit, which is the standard assumption in solid state theory, k becomes a continuous variable in the BZ. This is how one arrives at the m energy bands each being characterized by a continuous variable k and an index called the band index: $E_i(k)$, ($i = 1, 2, \dots, m$). The symmetry-adapted orbitals characterized by a k -vector are called crystal orbitals. Thus, HOMO is replaced by HOCO and LUMO by LUCO in the polymer or solid. If there is a finite energy separation between the top occupied band and the lowest empty band, the system has a forbidden band gap, or band gap, E_g .

The Fermi energy, E_F , is halfway between the HOO and the LUO at zero temperature. For metallic systems without a band gap, E_F represents the common HOO–LUO energy. Figure 2 illustrates the two-dimensional (2D) BZ of graphene, with the corresponding energy bands³⁰ and density of states (DOS).^{20b} The latter is proportional to the number of available states in an infinitesimal energy interval and condenses the complex energy band information into a one-dimensional graph. The DOS is zero within the band gap: There are no allowed states with those energy values. It is an interesting fact, which will play a key role in some of the discussions in this review that the DOS at E_F is zero²⁰ for graphene. At the Hückel level, the band gap is zero for graphene.

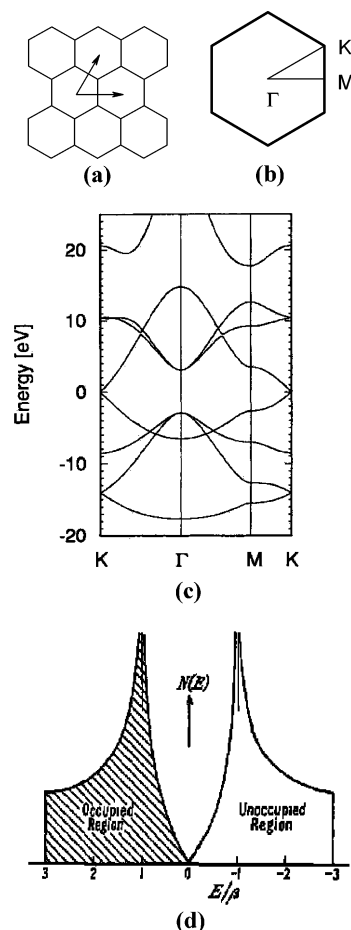


Figure 2. Geometrical and electronic properties of graphene. (a) Graphene unit cell, (b) BZ, and (c) band structure. Reprinted with permission from ref 30. Copyright 1992 American Physical Society. (d) DOS at the Hückel level. Reprinted with permission from ref 20b. Copyright 1952 Institute of Physics and IOP Publishing Ltd.

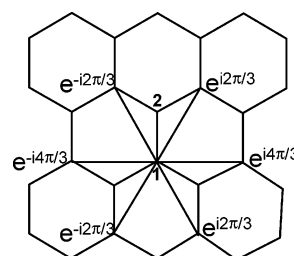


Figure 3. Phases of graphene orbitals for neighboring cells at the K -point in the BZ.

There are two degenerate states at E_F . The degeneracy occurs at a special point in the BZ, which is usually designated as the K -point. The corresponding wavefunctions at the Hückel level are indicated in Figure 3. These two orbitals are nonbonding at this level of theory, but they are slightly antibonding when second neighbor interactions are taken into account.³¹ This second neighbor interaction breaks the symmetry of the orbitals between the HOCO and the LUCO explaining the changes of the observed CC bond distances in positively and negatively doped or intercalated graphites.

2. Conjugated Molecules and Simple Extended Systems

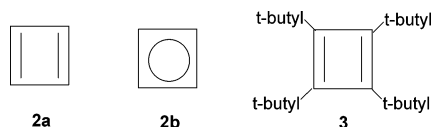
2.1. Jahn–Teller (JT) Effects in Conjugated Molecules

The distortive nature of π -electrons in many conjugated molecules may be understood by referring to the JT³² effect: The ground states of many molecules should not have the highly symmetric configuration expected on the basis of ordinary resonance theory but rather an unsymmetrical or a lower symmetry configuration as a result of the mixing between the ground and the excited electronic states coupled through the motions of the nuclei.

In this section, the electronic structures of four unique categories of conjugated systems where the JT or the pseudo-JT effect is operative are discussed. Note that the higher symmetry reference structure does not necessarily correspond to a minimum on the PES. It corresponds to a hypothetical molecular structure that provides a useful point of reference for the discussion.

2.1.1. Cyclobutadiene, an Open Shell System

Cyclobutadiene has alternating CC bond distances, **2a**, corresponding to a D_{2h} ground state.³³ However, the reliability of the experiments regarding the CC bond lengths has been scrutinized in view of the unexpected temperature dependence of X-ray data for tetra-*tert*-butylcyclobutadiene, **3**. At room temperature, these data indicated a very insignificant difference between the intracyclic CC bond lengths (1.482 and 1.464 Å).^{33c} At first, such a nearly square structure was thought to be due to the influence of the substituents,^{33d} but experiments at 123 K showed substantial alternation of the bond lengths ($\delta = 0.086$ Å)^{33e} and this unexpected temperature dependence of the structure was ascribed to some residual disorder possibly present even at 123 K. The anisotropic displacement parameter analysis of **3** showed that the data measured at room temperature correspond to an averaged superposition of two mutually perpendicular rings with strong BLA.³⁴



This BLA has been associated with the antiaromatic destabilization of cyclic conjugated molecules with $4n$ π -electrons. The corresponding potential surface along q , with a pair of degenerate localized ground state structures, is illustrated in Figure 1b.³⁵

This structural distortion toward a bond length alternating configuration in cyclic oligoenes with the composition of $C_{4n}H_{4n}$ is due to a JT distortion at the Hückel level. At a higher level of theory, the effect is more properly described as a pseudo-JT distortion. This term is used when structural distortion occurs due to the mixing of the near degenerate electronic states.³⁶ In the simple one-electron picture, cyclobutadiene in the high symmetric configuration, **2b**, possesses a pair of degenerate nonbonding orbitals,

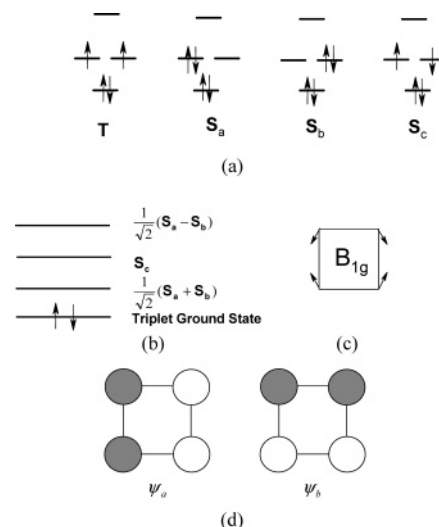
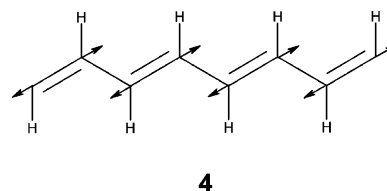


Figure 4. Electronic structure of cyclobutadiene. (a) Four possible electron configurations. (b) Four states. (c) The vibrational normal mode that mixes two singlet states. (d) Degenerate MO pair of symmetric cyclobutadiene.

to which two electrons are assigned, leading to an ordinary π -electron driven JT distortion at that level of theory. There are four main electron configurations and four states as shown in Figure 4a,b; a set of real nonbonding orbitals are shown in Figure 4d. In the one-electron picture, the triplet state is the ground state with a symmetric geometry. [Note that in order to describe the ground state of this system correctly, multiconfigurational wavefunctions such as complete active space self-consistent field (CASSCF)³⁷ with at least four π -electrons and four π -orbitals must be used. In fact, in the case of symmetric cyclobutadiene,³⁸ the ground state is ${}^1B_{1g}$, which corresponds to the S_c state, an open shell singlet state. In any case, symmetric cyclobutadiene has an open shell ground state.] Therefore, C₄H₄ is an open shell system before the geometric distortion is considered. In the one-electron picture, a pseudo-JT distortion occurs as the two singlet states [$1/\sqrt{2}(S_a + S_b)$, $1/\sqrt{2}(S_a - S_b)$] mix with each other through the b_{1g} normal mode (Figure 4c), which lowers the molecular symmetry from D_{4h} to D_{2h} . This particular mode stabilizes S_a, while it destabilizes S_b. Consequently, a singlet state that has a larger contribution from S_a ($c_1S_a + c_2S_b$, $|c_1| > |c_2|$) becomes the ground state. In other words, the normal mode mixes some of the higher energy $1/\sqrt{2}(S_a - S_b)$ state with the lowest singlet, thereby stabilizing it. Note that this mode largely consists of a simultaneous lengthening and shortening of alternating CC bonds around the ring, and it is analogous to the vibrational BLA mode of PA (**4**) and of other conjugated polymers mentioned in the Introduction.

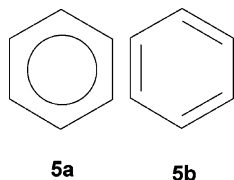


There have been quite a few theoretical studies³⁹ on the geometry of the ground state of cyclobutadi-

ene. Koseki and Toyota³⁸ discussed an energy component analysis by using MCSCF (multiconfiguration self-consistent field) theory³⁷ concluding that in the ground state of planar cyclobutadiene, the stability of a bond-alternated structure is largely attributable to the decrease of σ -electron effects and the concomitant increase of π -electron effects resulting in a D_{2h} structure. Recent geometry optimizations⁴⁰ with Becke's three parameter hybrid density functional, and Lee–Yang–Parr nonlocal correlation functional (B3LYP) density functionals for tetra-*tert*-butyl-cyclobutadiene, display very unequal bond lengths (1.354 and 1.608 Å) in agreement with the experimental conclusion that the low temperature X-ray structure was distorted. They further showed that the system is strongly antiaromatic based on magnetic and energy criteria.

2.1.2. Benzene, a Closed Shell System

Herzberg⁴¹ has established using vibrational spectroscopy that benzene has a D_{6h} structure with no bond alternation, $\delta = 0$ (**5a**). X-ray structural data for benzene are compatible not only with the crystallographically ordered D_{6h} (**5a**) structure but also with a disordered D_{3h} (**5b**) model associated with superposition of Kekulé type benzene molecules.⁴² Other studies, such as infrared and Raman spectra of gaseous benzene, neutron diffraction experiments of crystalline benzene, gas phase electron diffraction, and gas phase rotational spectroscopy, are equally incapable of resolving unambiguously the structure of benzene, according to Ermer's analysis.⁴² Therefore, it seems that current experimental techniques may not be able to definitely resolve the degree of bond alternation in the ground state of benzene.



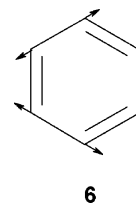
In contrast, all ab initio calculations⁴³ unequivocally point to a D_{6h} structure for benzene corresponding to a potential surface along δ , where only one minimum exists at $\delta = 0$, as illustrated in Figure 1a. This preference for a delocalized, nonalternating D_{6h} (**5a**) structure is widely considered as a symptom of aromaticity in benzene.

LHS⁴ showed that the antisymmetrical bond alternating distortion coordinate has b_{2u} symmetry, **6**, and it mixes the ground $^1A_{1g}$ π -electronic state with the excited $^1B_{2u}$ state. Because of the large energy difference between the two states, however, the mixing is small and lowering of π -electron energy is not sufficient to overcome the compression of the σ -bonds needed for making a D_{3h} structure more stable than a D_{6h} structure. Although benzene does not distort from a D_{6h} symmetry, the distortive tendency toward D_{3h} does exist in this representative aromatic molecule.^{44–46}

Why does benzene have D_{6h} symmetry? Does the D_{6h} structure originate from the additional stability

of the aromatic π -electrons or from the backbone of σ -bonds (electrons)? Shaik et al.^{46c} and subsequently Jug and Köster⁴⁷ have analyzed the structure of benzene by probing the distortive behavior of the π -electrons using modern methods. In the picture that emerges from these all-electron studies, the π -component enjoys resonance stabilization but is also distortive and prefers a D_{3h} symmetry, and it is the resistance of the σ -frame to the distortion that restores the D_{6h} structure. This viewpoint of benzene has been criticized by Glendening et al.,⁴⁸ cautioning that the energy partition within all-electron calculations is arbitrary and possibly misleading because it may involve an inherent bias toward π -distortivity. In response to this, Hiberty et al.⁴⁹ subsequently developed an approach termed the "quasiclassical state" allowing a further refinement of their original argument.

A convincing spectroscopic argument to support this view came from Haas and Zilberg.⁵⁰ They discussed the experimental frequency shift of the b_{2u} vibration, **6**, which is the bond alternation mode and analogous to **4**. This mode shifts *upward* by 260 cm^{-1} in the first excited state of benzene ($^1B_{2u}$ state), relative to the vibrational frequency of the similar mode in the ground state. They argued that the π - π^* excitation disrupts the delocalization of the π -electrons and weakens thereby the π -distortive propensity, leading to a higher not a lower frequency in the excited state. This weakening of the π -contribution should in turn reveal more clearly the influence of the σ -potential on the b_{2u} mode and lead to a frequency exaltation of this vibrational mode. Theoretical analysis of Shaik et al.⁵¹ further substantiated this interpretation of the experimental evidence. Independent supports for this viewpoint came also from further theoretical studies.^{52–55}

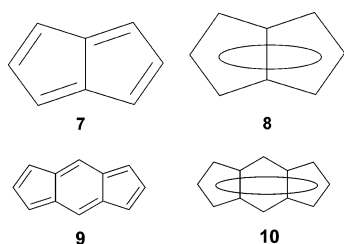


More detailed review of benzene can be found in other articles of the previous aromaticity issue.² The distortive tendency present in benzene is a second-order effect. How special is benzene in the series of $[4n + 2]$ annulenes? As the size of these $4n + 2$ π -electron systems increases, the gap between ground and low-lying excited states decreases. Therefore, one would expect that the distortive tendency becomes stronger in large annulenes (see section 2.3) linking this problem to the BLA in *trans*-PA.

2.1.3. Pentalene and *s*-Indacene, a "Quasi" Open Shell System

In probing the bond alternation properties of other $4n$ systems, pentalene (**7** and **8**) and *s*-indacene (**9** and **10**) offer further insights. If the transannular bonds can be considered as a minor perturbation to the peripheral conjugated carbon ring, both pentalene, **7/8**, and *s*-indacene, **9/10**, may be categorized as

normal $4n$ π -systems: antiaromatics with a potential surface where two degenerate localized ground state structures exist (see Figure 1b).



These molecules may be considered as “quasi” open shell systems where the lowest antibonding orbital is near the HOMO orbital at symmetric structure, **8** and **10**. [Note that in cyclic $4n$ π -electron systems ($C_{4n}H_{4n}$), the LUMO and HOMO orbitals are degenerate.] Such a low-lying antibonding orbital can mix with the HOMO orbital if the geometry is distorted along the b_{1g} normal mode, **11**, stabilizing the HOMO orbital. This mechanism leads to a BLA in pentalene. This is another pseudo-JT effect as illustrated in Figure 5a. In the case of *s*-indacene, the effect is

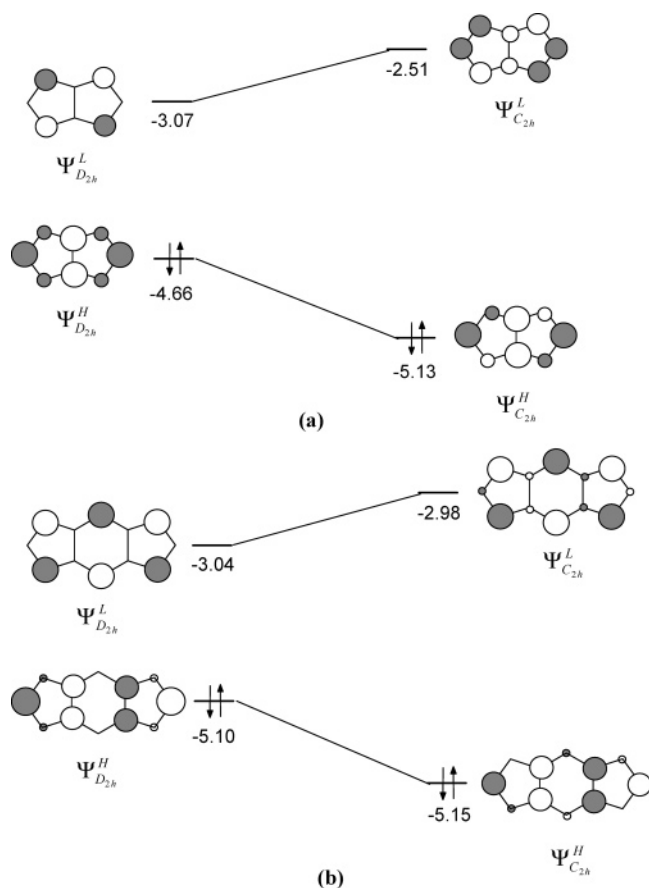
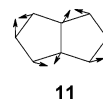


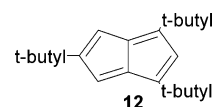
Figure 5. HOMO–LUMO gaps of the D_{2h} and C_{2h} structures of (a) pentalene and (b) *s*-indacene.

weaker due to a larger gap of 2.06 eV as compared to 1.59 eV of pentalene between the HOMO and the antibonding orbital at its symmetric structure (see Figure 5b) as calculated at the B3LYP/6-31G* level of theory.⁵⁶

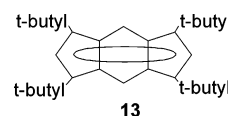
Interest in pentalene, **7/8**, was initiated by its proposed aromaticity.⁵⁷ Subsequent theoretical stud-



ies⁵⁸ suggested that localized pentalene (**7**) would be lower in energy but antiaromatic. X-ray analyses of 1,3,5-tri-*tert*-butylpentalene (TTBP, **12**) and 1,3-di-*tert*-butyl-4,5-dimethyl-carboxypentalene (DBMP)^{59,60} indicated a localized structure for the pentalene skeleton. Dynamical ¹³C NMR experiments⁶¹ indicated that the valence tautomerization barrier of **12** in solution at 93 K is 3.8 kcal/mol.



In contrast, the ground molecular structure of *s*-indacene is not clear. Low temperature X-ray analysis indicated that the substituted 1,3,5,7-tetra-*tert*-butyl-*s*-indacene (**13**)^{62,63} may have a symmetrical (delocalized) rather than a bond alternating (localized) structure.⁶⁴ In addition, the presence of only four ¹³C NMR signals for the 12 carbons in **13** at -130 °C also indicates the possibility of a symmetrical structure. This issue is of current interest in terms of both its derivatives⁶⁵ and *s*-indacene itself.^{66–68}



According to simple MO,^{69,70} semiempirical,⁶² and HF calculations,⁶⁷ the localized C_{2h} structure **9** with alternating C–C bond lengths around the ring perimeter is favored energetically relative to the D_{2h} “delocalized” structure **10**. Inductive perturbations of the alkyl groups might eliminate the energy difference between the two structures in **13**.⁴² Recent calculations by Hertwig et al.⁶⁶ have shown **9/10** to be a borderline case for bond localization. For example, HF, Møller–Plesset second-order perturbation theory (MP2), and CASSCF favored the localized **9**, and density functional with Becke 88 nonlocal exchange and Perdew 86 nonlocal correlation functional (LDA-BP)/triple- ζ polarized basis sets (TZP) and complete active space, second-order perturbation theory (CASPT2) yielded the delocalized **10**. On the basis of these results and the crystal structure of **13**, Hertwig et al.⁶⁶ concluded that the parent *s*-indacene should also have a delocalized structure and ascribed the high reactivity to a singlet diradical character. With the help of B3LYP/6-31G(d) method, Nendel et al.⁷¹ also concluded that *s*-indacene is a nonaromatic system with a fully delocalized geometry. Note that the model chemistry provided by the B3LYP/6-31G(d) method has proven quite reliable in this case.⁷²

As discussed, the relatively small structural distortive tendency of *s*-indacene can be attributed to the large HOMO–LUMO gap calculated at the symmetric structure. The large gap is due to the presence of two transannular bonds, which stabilize the HOMO without much affecting the LUMO orbital (see Figure

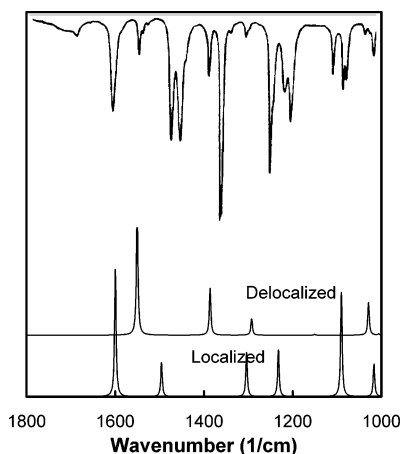


Figure 6. Calculated IR spectra of D_{2h} (delocalized) and C_{2h} (localized) structures of pentalene as compared with the experimental spectrum of TTBP. Reprinted with permission from ref 60. Copyright 1995 American Chemical Society.

5b). It is interesting to note that the calculated magnetic properties of this molecule do not seem to be sensitive to the **9/10** valence isomerization.⁷³

Choi et al.⁵⁶ showed correlation between the structure and the IR spectra of the localized and symmetrical forms, **7/8**, of pentalene. The calculated IR spectra of **7** and **8** demonstrated that the C–C and C=C stretching frequencies and intensities depend strongly on the structure, and the predicted vibrational pentalene⁶⁰ frequencies of **7** are in better agreement with experiment of tri-*tert*-butyl-pentalene (see Figure 6). In the case of *s*-indacene, a comparison with the experimental spectrum⁶⁷ of **13** showed that except for the peaks corresponding to the *tert*-butyl groups, the calculated spectra are in good agreement with experiment (see Figure 7). It is noted that there is very little difference between the

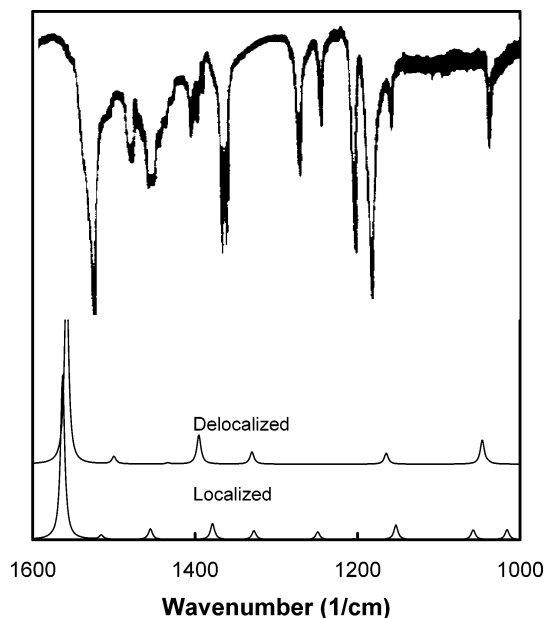


Figure 7. Calculated IR spectra of D_{2h} (delocalized) and C_{2h} (localized) structures of *s*-indacene as compared with the experimental spectrum of 1,3,5,7-tetra-*tert*-butyl-*s*-indacene. Reprinted with permission from ref 67. Copyright 1993 American Chemical Society.

calculated spectra of the symmetrical and the localized structures despite their substantial structural differences. The example of *s*-indacene shows that when the structural distortive tendency is small, some molecular properties do not depend strongly on the bond alternation tautomerism.

2.2. Peierls Distortions in Simple Extended Systems

2.2.1. PA, a One-Dimensional Extended System

As illustrated in Figure 8, $[4n + 2]$ annulenes approach the polymeric PA molecule, when n increases to infinity. Because $[4n]$ annulenes are JT systems, these also would approach the same limit at large N . Very long linear polyenes should have the same bond alternation properties as well.⁷⁴ The electronic structure of the symmetric form, **17**, which has equal bond lengths, has a zero band gap and should therefore be metallic. The properties of bond alternation resulting from the mixing of ground and low-lying excited states are very general. Peierls¹⁸ and others^{15–17,75} have shown that if a 1D solid has a half-filled band, it will always be unstable toward a distortion, which mixes energy levels above and below the Fermi energy eventually yielding one of

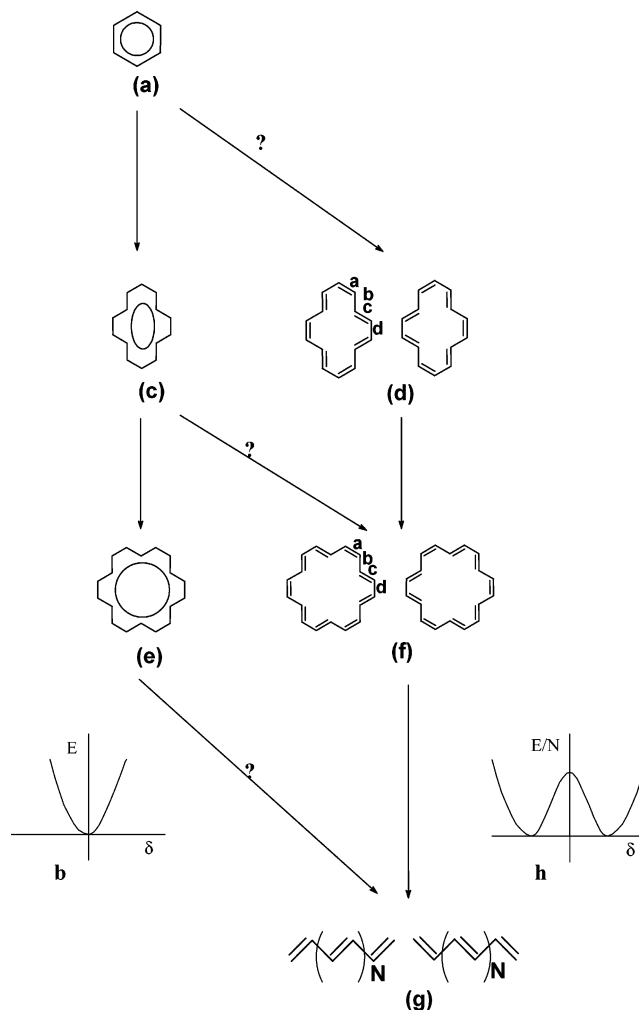


Figure 8. Alternative PESs of benzene, [14]annulene, [18]annulene, and PA along the q alternation coordinate. See text.

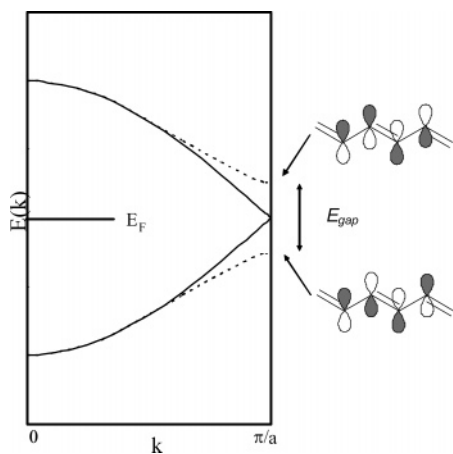
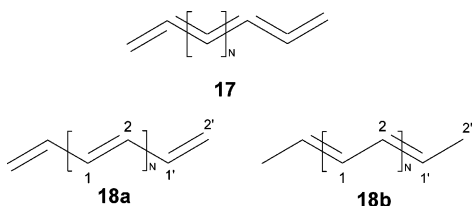


Figure 9. Band structures of bond length alternating (dashed line) and nonalternating (continuous line) geometries of PA. E_F is the Fermi level. Inserts show the splitting of the frontier orbitals after the BLA distortion takes place.

the lower symmetry structures **18**. The two lower symmetry structures are equivalent, constituting an example of a so-called degenerate ground state polymer. Although the actual value of δ in PA is still somewhat uncertain, the generally accepted range is 0.07–0.09^{76,77} Å. The associated band gap is around 1.5 eV.⁷⁸ Note that this alternation value is much smaller than what one obtains by HF geometry optimization. Furthermore, the band gap values calculated by HF are several times the experimental value.^{75a} These fundamental discrepancies between theory and experiment stimulated much research as discussed in this review.



The fact that the alternating structure should be more stable than the symmetrical nonalternating one can be understood by using a simple orbital argument concerning the energy of the highest occupied level, as illustrated in Figure 9. The advantage of this argument is that it can be easily extended to other systems, including ladder type polymers or heterocyclic polymers.

As the structure is being changed from symmetrical to unsymmetrical, along a generalized coordinate corresponding to the BLA mode,

$$q_{\text{BLA}} = a\delta = a(r_{\text{single}} - r_{\text{double}}), \quad -1 \leq a \leq 1 \quad (4')$$

the HOO is being stabilized on account of both gaining bonding character in the double bond region and losing antibonding character in the single bond region. The LUO undergoes a similar perturbation in the opposite direction, leading to a sizable band gap, E_g . The Peierls coordinate q_{BLA} provides a linear interpolation between a geometrical configuration with two equivalent bonds ($a = 0$) and one with the

fully developed single and double bonds ($a = 1$ or $a = -1$). Note that in reality other degrees of freedom, such as bond angles and CH bond distances, couple weakly to this mode.

Within non-SCF theories, such as simple Hückel theory, LHS theory, or extended Hückel theory, the band gap is proportional to the equilibrium value of the BLA coordinate^{18,79}

$$E_g = c_{\text{altern}} q_{\text{BLA}}^{\text{equ}} = c_{\text{altern}} (r_{\text{single}} - r_{\text{double}}) \quad (5)$$

The proportionality holds for small values of the distortion, showing the fundamental connection between the geometrical and the electronic degrees of freedom ($q_{\text{BLA}}^{\text{equ}} = \delta$ is the equilibrium value of the Peierls distortion). This connection, although significantly modified from the case of PA, remains a characteristic feature of many π -conjugated polymers.

The fundamental difference between the Peierls distortion and the JT distortion can be expressed in the dependence of the *total energy* for small values of the distortion parameter q (we are omitting the BLA index for simplicity). For the Peierls case, up to the lowest relevant order in q ,

$$E_{\text{Peierls}} = c_P q^2 \ln q + 1/2 k q^2 \quad (6)$$

while for the JT case

$$E_{\text{JT}} = -c_{\text{JT}} |q| + 1/2 k q^2 \quad (7)$$

The driving force toward distortion is only second order in the second-order JT (SOJT, or pseudo-JT) case:

$$E_{\text{p-JT}} = -c_{\text{p-JT}} q^2 + 1/2 k q^2 + K q^4 \quad (8)$$

In all three cases, the k (and K) terms represent the elastic contribution from the σ -bonds giving rise to the restoring force toward equidistant geometry ($q = 0$). (In the last case, distortion occurs if $-c_{\text{p-JT}} + k/2 < 0$; thus, the anharmonic Kq^4 term limits the distortion.) The distortion arises from the electron–nuclear coupling, which is linear for small q values in the JT case, but it has a logarithmic divergency in the Peierls case. Thus, in the JT case, the equilibrium value of the distortion parameter is

$$\delta_{\text{opt}} = c_{\text{JT}}/k \quad (9)$$

This value is larger if the electron–nuclear coupling is stronger or the restoring force constant is smaller.

In the Peierls case

$$\delta_{\text{opt}} = \text{const} \exp(-k/2c_P) \quad (9')$$

leading to a nonzero distortion. The logarithmic divergency is the result of the fact that in the infinite chain the bond alternation opens a gap in the band structure of the chain. Since this causes all levels in the vicinity and below E_F to be lowered (as illustrated in Figure 9), the driving force obtained in this manner qualitatively differs from the driving force obtained from a single isolated level, which is the case in the JT distortion. Obviously, for longer and longer

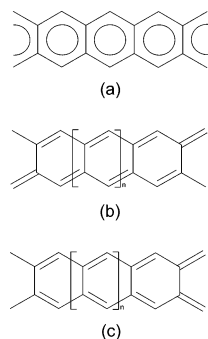


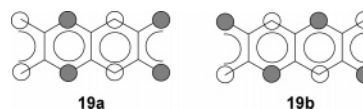
Figure 10. Three possible geometric structures of polyacene. (a) Metallic nonalternating structure. The two lower symmetry, bond length alternating structures are *trans*-polyacene (b) and *cis*-polyacene (c).

oligomers, an increasing number of levels near the frontier orbitals can be stabilized by the distortion, leading to a distortive force that becomes larger with increasing chain length, eventually giving rise to larger distortions for longer oligomers. We shall refer to this argument when discussing long polyenes in section 2.3.

2.2.2. Polyacene, a “Quasi” One-Dimensional Extended System

If we consider the transannular bonds as a perturbation like we did for *s*-indacene, **9**, then the electronic structure of the oligoacenes, **19** (oligomers of polyacene), may be derived from those of two parallel running PAs. The issue here is whether bond-alternating structures exist, as n increases toward infinity despite the coupling between the two PA-like “rails” of a ladderlike polymer. Polyacene, the hypothetical infinite system, has never been made so far, but it is an ideal target for theoretical studies^{80–83} with important implications for the study of small band gap extended polymeric systems and their PESs. Three possible forms of infinite polyacene are illustrated in Figure 10. In contrast to PA, there are two different lower symmetry nonmetallic structures (**b,c**) into which the metallic structure, **a**, can develop. LHS⁸⁰ discovered that bond alternation along the two edges would mix states of the same symmetry type but the large gap between these precludes a large energy gain. Whangbo et al.²⁵ have shown that the *trans* form (Figure 10b) is slightly more stable at the extended Hückel level, a conclusion supported by orbital interaction arguments. Compounds **19a** and **19b** show the two degenerate frontier orbitals obtained at the Hückel level for an infinite symmetrical polyacene. The phase differences between neighboring unit cells indicate that these orbitals are at the edge of the BZ, at $k = \pi/c$, where c is the translational vector. These orbitals are localized at the edge carbon atoms. Their predicted band gap values are in qualitative agreement with the experimental estimate of around 0.3–0.5 eV based on the extrapolated value of $\pi \rightarrow \pi^*$ transitions of finite oligoacenes.⁸⁴ Čížek and Paldus have suggested that in long oligoacenes “singlet instabilities” of the HF equations may occur.⁸⁵ Different levels of calculations predict that one of the nonmetallic structures is slightly more favorable by a few tenths

of a kcal/mol.⁸⁶ Kertesz and Hoffmann⁸¹ showed that the system gains stabilization energy from the interaction between a partially filled band and an unoccupied band separated by a few electronvolts, as opposed to the Peierls situation, where the mixing is at the Fermi level. Recently, Raghu et al.⁸⁷ have shown within the π -only PPP Hamiltonian but including correlation effects, the Peierls distortion in polyacene is enhanced by the inclusion of electron correlation and that the *cis*-form of the bond alternation is favored in agreement with the modified neglect of diatomic overlap (MNDO) CO results.^{86b} The decreased tendency of bond alternation for oligoacenes relative to PA has implications for the structure of single wall carbon nanotubes (SWCNs). (For a connection to graphite, which has uniform CC bonds, see subsection 2.2.3.)



A recent report⁸⁸ predicted that the aromaticity of each of the benzene rings in cyclacenes (these are rolled up oligoacenes in a cylindrical fashion akin to those of a “belt” of a SWCN) with 5–14 benzene rings was reduced by the strain of the cyclic system. Türker also explored cyclacenes with the semiempirical molecular orbital (MO) method, Austin model 1 (AM1), but he mainly discussed the MOs as a function of size and the convergency of the energy gap as the size of the linear and cyclic oligoacenes was increased.⁸⁹

For longer polyacenes and for cyclacenes, (U)-B3LYP/6-31G* calculations by Houk et al. indicated that their ground state becomes a triplet state as the oligomers size is increased.⁸³ They concluded that the geometries of polyacenes and cyclacenes have two fully delocalized nonalternating ribbons joined by relatively long bonds (transannular bond). The analogy with *s*-indacene was also emphasized in this study. The (U)B3LYP geometry optimizations were followed by time-dependent density functional theory (TDDFT) calculations for the singlet–singlet gaps, yielding S_0 – S_1 singlet–singlet transition energies for the $\pi \rightarrow \pi^*$ absorption that gradually decrease reaching 0.80 eV for the oligomer with nine rings, the largest cyclacene studied. This value is consistent with the available experimental excitation values obtained for linear oligoacenes mentioned above.⁸⁴ S_0 – T_1 singlet–triplet gap values calculated by the TDDFT method indicated that singlet–triplet gap gradually decreases as the size increases and the triplet state becomes the ground state at a particular size of polyacene. Recent density functional theory (DFT) and CASSCF calculations at UCLA⁹⁰ indicated that the BLA is suppressed in polyacene,⁸³ and for long oligoacenes, an open shell singlet is the predicted ground state. According to Bendikov et al., the singlet diradical state becomes the ground state for oligoacenes longer than hexacene. The nature of the diradical is such that the two electrons are localized on the opposing edge carbons of the two PA-like chains, which are then connected by longer, sp^2 – sp^2

transannular bonds. Note that these are finite molecules, not infinite chains; nevertheless, they are directly related to the Hückel level orbitals for the latter (**19a,b**). The excited states of oligoacenes with up to 10 rings have been studied with highly correlated methods but within the π -electron only PPP Hamiltonian.⁹¹ Both the ab initio and the semi-empirical studies obtained reasonable excitation energies.

A more complete understanding of the structural trends in polyacenes that represent bridges between *trans*-PA and graphene is essential for understanding aromaticity. Another route to approach the graphene limit starting from various polycyclic aromatic hydrocarbons and reaching as many as 91 conjugated aromatic benzene rings has been reviewed by Watson et al.⁹² The largest of these systems have a moderate band gap below 1 eV. These systems indicate that there are various routes toward graphene. Polyphenanthrenes provide another link between a single PA chain and ladderlike linked architectures that extend into the second dimension.⁹³ However, these systems have much larger band gaps and very uneven bond distances with significant bond localization.⁹⁴ These contrary trends leave the question open as to which sequence of oligomers is representative in describing the uniform bond distances and semimetallic properties of graphene.

2.2.3. Graphene, a Two-Dimensional Extended System

All CC bonds in graphite have the same length of 1.421 Å.⁹⁵ Presumably, the same holds for the CC bonds in a 2D layer of graphite, graphine, because the interlayer interactions do not significantly change intraplane bonding.⁹⁶ The electronic driving forces toward possible distortions from this equidistant geometry in graphene have been studied by Anno and Coulson at the level of theory that included only a Hückel electronic term and a σ -electron elasticity term.⁹⁷ They have shown that within a wide range of plausible parameter choices the lattice maintained uniform CC bond distances. They considered only a limited number (three) of periodic distortion patterns in their numerical study. These distortions lower the symmetry of the lattice and increase the size of the unit cell. Anno and Coulson related the stability of the equidistant lattice toward these symmetry lowering distortions to the density of orbital levels near the Fermi surface. (See also the discussion on p 504 of Salem's book.⁷⁴) Although graphene has a zero band gap, a vanishing density of orbital levels near the Fermi energy would not provide the driving force for any CC BLA.⁹⁸ Recent calculations in our laboratory by S. Yang have shown that the conclusions of Anno and Coulson remain valid when using ab initio density functional techniques and a number of different distortion patterns.⁹⁹

The tendency for a diminishing driving force when moving from one dimension (*trans*-PA) to graphene through polyacene and other ladder type systems provides further insight.⁸¹ Accordingly, the driving force toward alternation is reduced by fusing further chains to the ladder, continuing the construction from PA to polyacene to graphite. The gaps thus generated

diminish with each fused chain, eventually leading to no distortion in the 2D limit. Lack of Peierls distortion for metallic SWCNs will be discussed next.

2.2.4. SWCNs and Their Geometrical Properties

A different aspect of this problem came up in the context of investigating the propensity of SWCNs toward bond alternation due to a possible Peierls distortion of these highly conjugated carbon networks.¹⁰⁰ While SWCNs can be viewed as rolled up sheets of graphene, their quasi-1D architectures dictates that, at least formally, the tendency of metallic nanotubes toward Peierls distortion must be considered. Single wall nanotubes are characterized by the roll up vector $R = na_1 + ma_2$ (a_1 and a_2 are the lattice vectors of the graphene sheet, and n, m are integers). At the Hückel level of theory, SWCNs are classified^{100,101} as "metallic" ($n-m$ is divisible by 3, zero calculated band gap) and "nonmetallic" ($n-m$ is not divisible by 3, nonzero calculated band gap). It turns out that electronic structure calculations and experimental data confirm this pattern with significant exceptions from the Hückel-based rules only for small diameter ($D < 1$ nm) tubes. It is expected that nonmetallic tubes lack Peierls distortion. However, metallic tubes have substantial densities of states at the Fermi level, and some, albeit small, Peierls distortion is expected. These small distortions ought to lead to small band gaps, which should affect all properties, including electron localization, some loss of aromaticity, and changed chemical reactivity. Mintmire et al. and Saito et al. found no Peierls distortion.¹⁰⁰ More recent calculations indicate that the Peierls distortion for nanotubes should be very small, of the order of 1K (10^{-4} eV) for small diameter tubes.¹⁰² A calculated static band gap of 1K has to be evaluated in conjunction with quantum fluctuations and temperature effects. For large diameter tubes, even smaller gaps are expected, since the geometrical and electronic properties of nanotubes are very similar to those of graphene in the limit of large diameters. The small Peierls band gap can be rationalized by considering that there is only one band where the gap opening provides energy gain, while one needs to distort many σ -bonds. As compared to PA, there are more σ -bonds to distort, and the energy gain is much smaller due to the smaller bandwidth, which is a result of "band backfolding".²⁸ This leads to a several order of magnitude reduction of the Peierls gap.

Different kinds of bond distortions have been obtained in recent ab initio calculations by Kanamitsu and Saito¹⁰³ and Sun et al.,¹⁰⁴ who found that the bond distances in small radius nanotubes are not uniform. These deviations do not create a band gap, and they are not disrupting the Hückel based pattern as to which tubes should be metallic or nonmetallic. The deviations from uniform bond distances are small, of the order of a few picometers, but are systematic and closely related to the metallic or nonmetallic nature of the tubes and correlate with the divisibility by 3 rules mentioned above. This finding echoes the viewpoint that small radius nanotubes behave as individual molecular species with

different properties, such as different band gaps, geometries, etc.¹⁰⁵ It remains to be seen how the predictions will be reflected in the more selective experiments done on monodisperse nanotubes. These deviations of bond distances from uniformity are analogous to those observed for other aromatic molecules, such as naphthalene.

2.3. Transition of Bond Alternation as a Function of Size: [14]- and [18]Annulenes, Closed Shell Systems with Low-Lying Excited States

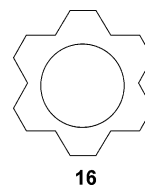
Properties of molecules evolve as the system size increases. This issue becomes particularly important with the advances of nanomolecular science. Figure 8 indicates schematically that as the size of the $C_{4n+2}H_{4n+2}$ annulene increases, it more and more resembles PA and should assume a bond alternating structure. At which critical n -value does the switch over from delocalized, benzenelike to localized, PA-like structure occur? What is the degree of bond alternation of the localized forms as a function of size? How do the molecular properties as a function of size behave for the localized and delocalized valence tautomers? How does the interplay of ASE (aromatic stabilization energy) and the JT effect determine the ground state molecular structures of large annulenes? The issue is only relevant for the $4n + 2$ series. The members of the $4n$ series, which are open shell systems in their high symmetry geometries, have a tendency for localization for all values of n , due to the strong pseudo-JT effect that stabilizes one of the low-lying singlet states more than the triplet ground state.

LHS studied the general problem of the equilibrium of cyclic $C_{4n+2}H_{4n+2}$ polyenes within the framework of simple Hückel theory in which σ -bond compression has been included.⁴ Using two different resonance integrals β_1 and β_2 for two of the different bond lengths, they have shown that for large n , the symmetric configuration becomes unstable. The “transition” to the bond alternating structure in $C_{4n+2}H_{4n+2}$ annulenes was predicted to occur around the critical n value, $n_{cr} = 8$ and $\delta = 0.036 \text{ \AA}$ ($R_{single} = 1.423 \text{ \AA}$ and $R_{double} = 1.387 \text{ \AA}$). Platt¹⁰⁶ and Labhart¹⁰⁷ showed that the same phenomenon can be explained for long polyenes by mixing of the ground state with low-lying excited states of proper symmetry.

After these predictions, further theoretical calculations have been done yielding different predictions for the critical n_{cr} value at which the transition occurs. Buss¹⁰⁸ showed that [18]annulene should have a marked density alternation indicating BLA. Fratev et al.¹⁰⁹ obtained analytical expressions for $4n$ and $(4n + 2)$ annulenes. They concluded that no bond alternation should occur for the first few members of $(4n + 2)$ series up to [30]annulenes. On the basis of a PPP–Hubbard¹¹⁰ Hamiltonian, Lieb and Nachtergaele¹¹¹ proved that the energy minimizing configuration of cyclic $(CH)_{2n}$ systems always has a repeat period of two π -centers when n is odd. When n is even, a new instability may destroy the periodicity of two as long as n is not too large. Recently, Buck¹¹² showed that when the degenerate HOMO does not contribute any more to the overall bond order values,

the π -electron system is forced to select a lower symmetry resulting in BLA. Nakajima^{10e} found that [18]annulene is stable against distortion into a structure with bond alternation, while [30]annulene is not.

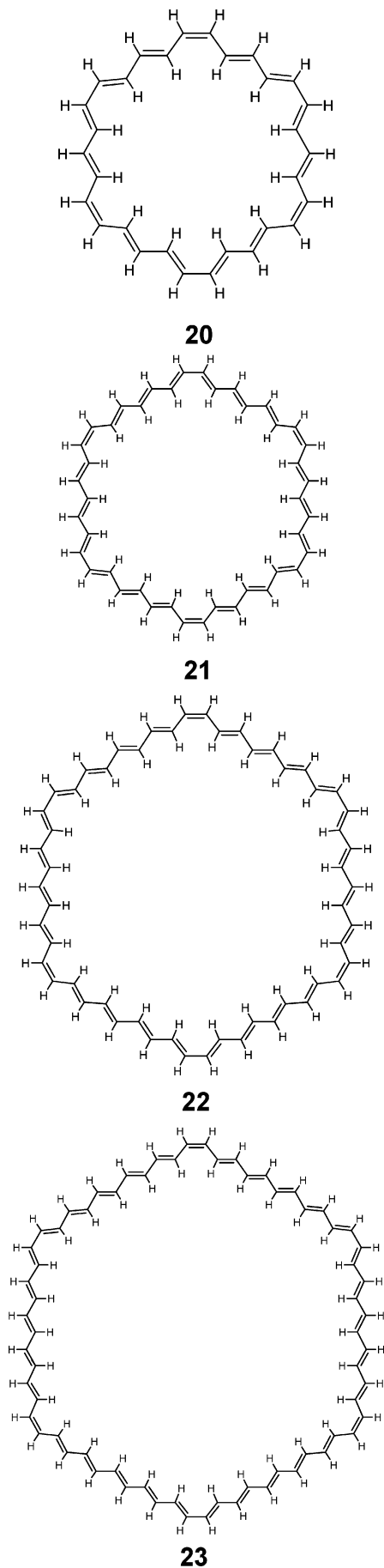
As the system size increases, a methodological problem known as HF instability arises. Čížek and Paldus¹¹³ derived the so-called HF stability condition and concluded that delocalized $[N]$ annulenes are unstable when $N \geq 14$. If the HF solution is unstable, the one-electron approximation is not adequate; therefore, electron correlation effects must be taken into consideration.



Using the semiempirical electron correlated modified neglect of diatomic overlap (MNDOC) (C for correlation) method, Yoshizawa et al.¹¹⁴ studied the geometrical and electronic structures of [18]- (**16**), [30]- (**20**), [42]- (**21**), [54]- (**22**), and [66]annulenes (**23**), which belong to a subgroup of aromatic $(4n + 2)$ π -electron systems and could exhibit a delocalized D_{6h} symmetry. They observed that the BLA widens the HOMO–LUMO gap leading to their stabilization within the one-electron approximation. However, the second-order energy (due to the electron correlation effects) is larger in the high symmetry D_{6h} structures, due to the smaller HOMO–LUMO gap. As a result of these competing factors, they found that for [18]annulene, the D_{6h} structure should be more stable by 6.4 kcal/mol, while for [30]annulene, the lower symmetry D_{3h} structure should be more stable by 4.6 kcal/mol.

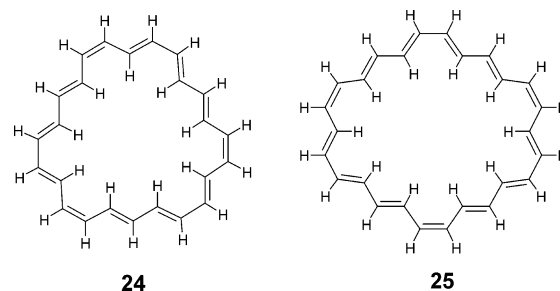
However, the question regarding the shape of the potential surface at the structural transition and corresponding consequences for molecular properties was not addressed: Is there a possibility that in addition to the two localized (Kekulé) structures there is yet another delocalized structure as a local minimum? Figure 1a describes the qualitative shape of the potential energy for benzene, while Figure 1b represents the PES for long annulenes. The crossover might occur via an intermediate potential surface, such as in Figure 1c. Only if this was the case, could one strictly speaking compare localized and delocalized structures of the same system. Paldus and co-workers¹¹⁵ found that the “transition” from single minimum, Figure 1a, to two minima, Figure 1b, occurs at [14]annulene without the intermediate situation displaying three minima.

Choi and Kertesz¹¹⁶ have performed calculations for up to [66]annulene {including [22] (**24**) and [26] (**25**)} using ab initio and DFT methods and compared the calculated alternation with the corresponding values for linear oligoenes. They studied the existence of a “structural transition” and corresponding asymptotic behavior of molecular properties as a function of size. According to the B3LYP results, the bond localization begins at [30]annulene with the δ value



of 0.035 Å. These results are very close to the early structural prediction by Longuet-Higgins and Salem,

especially for the critical n_{cr} value. According to subsequent ab initio calculations by Wannere et al. at a number of theoretical levels,¹¹⁷ the transition occurs at a smaller value, and alternation begins at [14]annulene. While the calculations are not decisive alone, the calculated proton chemical shifts are much more consistent with an alternating model for both [14]- and [18]annulene. At the same time, the X-ray data are consistent with both alternating and non-alternating structures.



The equilibrium δ values as a function of reciprocal size ($1/N$, where N is the number of carbon atoms) are collected in Figure 11 at different levels of theory. The three δ curves of $[4n + 2]$ annulene, $[4n]$ annulene, and polyene⁷⁷ (oligomers of *trans*-PA) series approach to the same limiting value of 0.05–0.06 Å. Choi et al. pointed out that the structural “transition” to the localized form via JT effect occurs when the HOMO–LUMO gap is lower than or close to 2 eV at the B3LYP level of theory. The limiting value of gap after the JT distortion of $4n + 2$ series approaches 1.1 eV, which is in good agreement with the experimental value for PA, 1.5 eV.^{78,118} Note that many variants of currently popular DFT parametrizations yield band gaps that are too small, typically by 10–20%. Certain hybrid density functionals are better and can in fact be calibrated to provide even better predictions for the band gap.¹¹⁹

Recently, Fokin et al.¹²⁰ studied imaginary $[N]$ -trannulenes, annulenes that have uniform shapes,

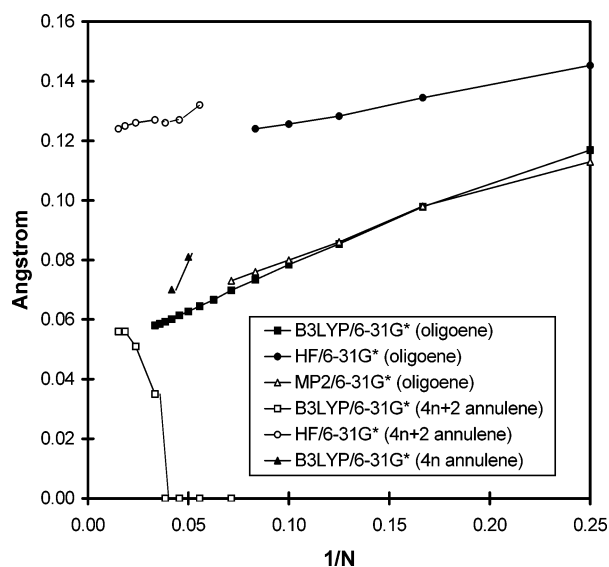
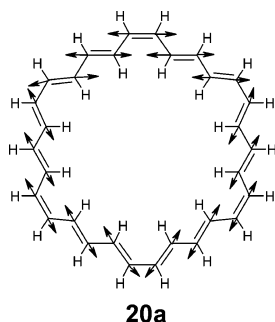


Figure 11. Optimized δ values of oligoenes, $[4n + 2]$ -annulenes, as a function of size ($1/N$, where N is the number of carbon atoms).

zigzag (trans) carbon rings, like a belt of rings of a "buckytube". When N goes to infinity, this series should also converge to PA implying structural transitions in this series. With B3LYP/6-31G* method, they observed the alternation with [30]trannulene that is fully consistent with the above result.

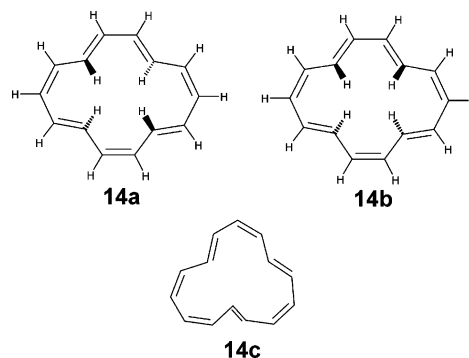
Normal-mode analysis informs about the presence or absence of a stable minimum. According to Yoshizawa et al.,¹²¹ in contrast to benzene and [18]annulene, the D_{6h} structure of [30]annulene has one imaginary b_{2u} mode at the B3LYP/6-31G** level. This mode, **20a**, calculated at $461 i \text{ cm}^{-1}$, confirms that high symmetry structure is in fact transition state. This mode corresponds to the Kekulé (BLA) coordinate. Note that this level of theory is deemed as reliable for investigating the structures and vibrational properties of aromatic systems.¹²²



[14]- and [18]Annulenes are $(4n + 2)$ π -electron systems, which more or less retain molecular planarity in their ground state structures as compared to the more strained and therefore less planar [10]-annulene. They are closed shell systems at their symmetrical structures ($\delta = 0$). The energy gap between ground and excited states decreases as system size increases. Thus, it is expected that the tendency toward bond alternating structure due to the pseudo-JT effect is stronger in these annulenes than in benzene.

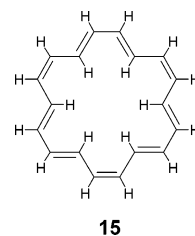
As prototypes of large annulenes, a great deal of work has been devoted to the study of these two annulenes in order to determine their structures and aromaticity. In the case of [14]annulene, the effect of the inner hydrogens on its structure has been thought to be large due to the short distances between these hydrogens. Early room temperature NMR^{123,124} was interpreted as resulting from two interconverting conformational isomers, **14a** and **14b**. However, Oth^{125,126} later concluded that [14]-annulene exists in solution as an equilibrium mixture of two configurational isomers [14]-43- (**14a**) and [14]-21-annulene (**14c**). From the chemical shifts of the inside protons, it was concluded that in **14a** the π -electrons are delocalized, although the perimeter must be appreciably distorted from planarity. Vogler¹²⁷ supported this argument on the basis of the ring current calculations taking into account local anisotropies.

X-ray data¹²⁸ showed that the molecule is centrosymmetric, **14a**, and significantly nonplanar with the four central carbon atoms displaced in pairs by 0.206 and -0.209 \AA above and below the average plane of the 14 C atoms. The C–C bond lengths vary



between 1.350 (11) and 1.407 (11) \AA . They found that it is aromatic with significant nonplanarity originating from the steric hindrance of the four internal hydrogen atoms.

Nevertheless, one should not forget that the X-ray diffraction could reflect an average of more than one π -bond localized situation, especially if the crystal is analyzed at room temperature. In fact, Choi et al.¹²⁹ argued that the 1.350 \AA value is too small to be an aromatic C–C bond length because it is equal to the minimum bond length of nonaromatic molecules.¹³⁰ The problems with this crystal structure are likely due to the small number of reflections in the data. Analysis of complete neglect of differential overlap/spectroscopic parametrization (CNDO/S)-configuration interaction (CI) calculations and the respective UV/vis¹²⁵ and photoelectron (PE) spectra¹³¹ brought further support to the delocalized C_s structure of [14]-annulene. The structural alternatives for the other prototypical annulene, [18]annulene, **15/16**, and its related aromaticity have also been extensively studied. Most experiments such as X-ray,^{132,133} heat of formation,¹³⁴ photoelectron spectroscopy,¹³⁵ and UV/vis¹³⁶ are consistent with a D_{6h} structure, **16**. Although earlier theoretical studies^{137–140} found that the bond alternating D_{3h} structure, **15**, might be more stable, later electron correlated calculations^{114,141–145} indicated that the D_{6h} , **16**, structure is the more favorable of the two.



According to ab initio calculations, HF geometry optimization¹²⁹ gives the localized C_s structure as the minimum, whereas some electron correlated methods such as Becke exchange with Lee, Yang, Parr correlation functional (BLYP), B3LYP, and MP2 favor a less alternating delocalized C_s structure. Wannere et al.¹¹⁷ have recently reported optimized geometries for [14]-, [18]-, and [22]annulenes at different theoretical levels. The geometry optimizations for [14]-annulene show strongly alternating structures at the HF, Kang–Musgrave hybrid density functional (KMLYP), and BHLYP levels of theory. On the other hand, a much less alternating geometry was obtained

by using B3LYP in agreement with previous calculations at that level. (The optimized structures do not include completely nonalternating models; because of ring strains, such a structure is not a minimum.) The key point that Wannere et al. make is that calculated proton chemical shift values based on the alternating models are in much better agreement with the experiment¹⁴⁶ than those based on less alternating or nonalternating (equalized) models. Very accurate quantum mechanical calculations including electron correlation, such as MP2 and coupled-cluster, singles and doubles with approximate triples [CCSD(T)], were also employed in this study but only at the geometries optimized at the lower levels of theory. Their MP2 results indicated, together with earlier calculations at that level, that the equalized structures are favored, but the more reliable CCSD(T)¹⁴⁷ results prefer the strongly alternating structures by 2–3 kcal/mol for [18]annulene. These energy differences are small, and the NMR experimental evidence was critical in the conclusion of Wannere et al. preferring the alternating form of [14]- and [18]-annulene. According to their conclusions,¹¹⁷ the alternation in the $[4n + 2]$ annulene series begins with [14]annulene; therefore, the sequence of stable structures should be **a** to **d** to **f** to **g** in Figure 8.

Vibrational frequencies can be another indicator of bond alternation as discussed in the previous sections, although extracting geometrical information from vibrational spectra is by no means unequivocal. Nevertheless, the agreement with the experimental IR spectrum is worse with a strongly alternating structure based on the HF geometry, as compared to the one obtained with an essentially nonalternating B3LYP geometry.¹²⁹ We have also calculated the vibrational frequencies at the BHLYP bond-alternating minimum structure (C_s).¹⁴⁸ A strong peak dominates the calculated spectrum at 1041 cm^{-1} (C–H out-of-plane bending), while this is a minor peak in experiment. In fact, the C_s structure as obtained with the BHLYP is nonplanar, which can generate a large dipole moment change for out-of-bending modes. It seems that further experimental and theoretical studies are needed to resolve this issue.

It is interesting to note that the relatively less widely used density functional KMLYP produces a geometry that is less alternating than that obtained by HF but more alternating than that obtained by B3LYP. These three methods, together with BHLYP and other similar methods, can be viewed as hybrid functionals with different percentages of exact exchange. (HF is a limiting case with 100%.) The degree of alternation is increasing with increasing exact exchange content in the energy expression, as will be discussed in section 2.4. This theme will be discussed in more detail in sections 3.1 and 3.4, as it has significant implications in choosing the appropriate model chemistries for conjugated polymers, whose band gaps are closely related to the magnitude of BLA mentioned in the Introduction.

Previously unobserved, nearly degenerate, isomeric forms of [16]- and [18]annulenes that differ in the spatial arrangement of the internal hydrogens and their internal C–C–C bond angles were observed

recently,¹⁴⁶ adding new aspects to the traditional understanding of aromaticity. Paratropicity and diatropicity in [16]- and [18]annulene are quite sensitive to the steric interactions involving their respective internal protons. Theoretical analysis of these effects on the degree of bond alternation would be of interest in further understanding the properties of annulenes.

2.4. Alternation, Exchange, and Band Gap

Nonlocal exchange plays a central role in many hybrid DFT calculations, especially for systems where BLA is important. We will first review the relationship between BLA and exchange for the case of PA, where it appears in a rather pure and direct manner. The presence of exchange modifies the relationship between alternation and band gap as given in eq 2 for the case of HF type π -electron Pariser–Parr–Pople (PPP) model.¹⁴⁹ The Fock matrix elements can be expressed as:

$$F_{rs} = H_{rs}^{\text{core}} + \sum_{t=1}^b \sum_{u=1}^b P_{tu} [(rs|tu)] - 1/2 (ru|ts) \quad (10)$$

where, H_{rs}^{core} represents the one-electron core Hamiltonian matrix elements, P_{tu} is the bond order matrix elements, and the two electron repulsion integrals are defined as:

$$(rs|tu) = \int \int \chi_r^*(1) \chi_s(1) \chi_t^*(2) \chi_u(2) / r_{12} \, dv_1 \, dv_2 = \langle \chi_r(1) \chi_t(2) | 1/r_{12} | \chi_s(1) \chi_u(2) \rangle$$

Here r , s , t , and u index the different atomic π -orbitals. According to the PPP model, σ – π separation and zero differential overlap (ZDO) approximation apply:

$$\chi_r^*(1) \chi_s(1) \, dv_1 = 0, \text{ for } r \neq s, \text{ and } (rs|tu) = \delta_{rs} \delta_{tu} (rr|tt) = \delta_{rs} \delta_{tu} \gamma_{rt} \quad (11)$$

which lead to diagonal and off-diagonal Fock matrix elements as:

$$F_{rr} = H_{rr}^{\text{core}} + \sum P_{tt} \gamma_{rt} - 1/2 P_{rr} \gamma_{rr} \quad (12)$$

$$F_{rs} = H_{rs}^{\text{core}} - 1/2 P_{sr} \gamma_{rs} \quad (13)$$

The next step is to apply the above equations to the PA system. In PA, allowing for two different bond distances, these indices can take on the values of 1 and 2 in each unit cell. (Prime refers to orbitals in an adjacent unit cell as in formula 18.) Within the first neighbor approximation and using PBCs, as discussed in the Introduction, k -dependent Fock matrix elements are obtained.²² For instance,

$$F_{21}(k) = F_{12} + e^{ik} F_{21'} = (H_{12}^{\text{core}} - 1/2 P_{12} \gamma_{12}) + e^{ik} (H_{21'}^{\text{core}} - 1/2 P_{21'} \gamma_{21'}) \quad (14)$$

The direct band gap occurs at $k = \pi$, and the band gap can be expressed as:

$$E_g = |2(H_{12}^{\text{core}} - H_{21'}^{\text{core}}) + (P_{21'}\gamma_{21'} - P_{12}\gamma_{12})| \quad (15)$$

At Hückel level, the nonlocal exchange term in eq 15 is absent, leading to a version of eq 2, assuming an exponential dependence of the resonance integral on bond distance:

$$E_g \approx |2(H_{12}^{\text{core}} - H_{21'}^{\text{core}})| \approx 2|\beta_0| |\exp(-\alpha r_{12}) - \exp(-\alpha r_{21'})| \approx 2|\beta_0| \alpha |r_{21'} - r_{12}| \quad (2'')$$

Beyond Hückel level, as in eq 15 of the PPP-SCF theory, the second term is nonzero. It comes from the bond order alternation wave¹⁵⁰ and leading to a nonzero gap even at the nonalternating geometry. Its value is

$$E_g(\delta = 0) = |P_{21'}\gamma_{21'} - P_{21}\gamma_{12}| = |P_{21'} - P_{21}| \gamma_{12} \quad (15')$$

The two bond orders $P_{21'}$ (intercell) and P_{21} (intracell) remain different even in the limit of $\delta = 0$, which is a reflection of a broken symmetry HF solution.¹¹³ A further metallic solution of the SCF equations also exists for the equidistant PA,¹⁵⁰ but it is "singlet unstable",¹¹³ signaling a propensity to a Peierls distortion. For such a metallic solution, $P_{21'} = P_{21}$, and $E_g(\delta = 0)$ is zero.

From a practical point of view, the alternating case is more relevant. In that case, the band gap has a large, relatively constant component coming from the exchange term and another that is approximately linear in δ . This feature can be also recognized in any theoretical model, where the exact exchange is included, such as B3LYP. Actual B3LYP calculations with fixed values of BLA are shown in Figure 12, where a sizable band gap is seen even at $\delta = 0$. This relationship between E_g and BLA is essentially linear when calculated at the B3LYP level with constrained alternating geometry of PA.¹¹⁹ This approximately linear relationship indicates that the band gap remains strongly dependent on the degree of BLA at levels beyond Hückel theory that include nonlocal exchange. (The relationship is very different from the one predicted for the effect of correlation on the gap by eq 3.) However, for theoretical models that do not include nonlocal exchange, the band gap of PA is calculated to be unrealistically small. There are quite a few publications in the literature that reflect this problem of underestimating both the optimized BLA and the corresponding band gap value, mostly due to this inadequacy present in a large class of density functionals.⁷⁷ Hybrid exchange, if the exchange content is carefully chosen, can overcome this difficulty.^{77,151} Assuming that the exact exchange content is $A_x < 1$, the corresponding gap will be reduced accordingly to this approximate formula:

$$E_g(A_x) \approx |2(H_{12}^{\text{core}} - H_{21'}^{\text{core}}) + A_x(P_{21'}\gamma_{21'} - P_{12}\gamma_{12})| \quad (16)$$

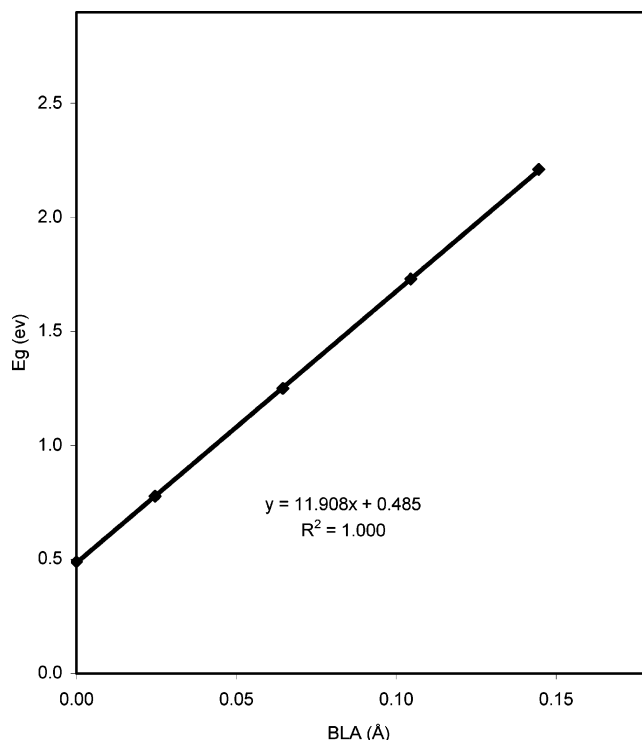


Figure 12. Relationship of band gap (E_g) and BLA in PA, obtained with B3LYP/6-31G* calculation with constrained geometry and from oligomer extrapolation method. Reprinted with permission from ref 119. Copyright 2004 Elsevier B.V.

For any given alternation value, one can find an A_x that adjusts the band gap close to the experimentally observed range. Choi et al.⁷⁷ have investigated the dependence of the bond alternation and band gap for polyenes by varying the exact exchange content of the following density functional: (this is the Becke's one parameter hybrid functional,¹⁵² B1)

$$E_{xc} = E_{xc}^{\text{DFT}} + A_x(E_x^{\text{HF}} - E_x^{\text{DFT}}) \quad (17)$$

The optimized bond alternation values depend very sensitively on A_x as it was varied from 0 to 1, covering a range of 0.065–0.12 Å for δ in the case of the $C_{10}H_{12}$ molecule. The dependence of the gap on A_x is even more pronounced producing gaps between 2 and 8 eV for $C_{10}H_{12}$. A_x values around 0.2–0.6 provided reasonable alternation and gap values. It is worthwhile to note that one of the popular Becke three-parameter exchange (B3) density functionals¹⁵³ contains 20% nonlocal exact (HF) exchange.

For the opposite reason, theories that rely on a variant of full nonlocal exchange HF theory ($A_x = 1$) systematically overestimate the band gap of PA and of all other conjugated polymers. These methods include widely used semiempirical techniques, such as AM1, modified neglect of diatomic overlap-parametrization method 3 (PM3), and Zerner's version of the intermediate neglect of differential overlap (ZINDO), neither of which is therefore recommended for band gap calculations of conjugated polymers. Comparisons of various representative theoretical approaches as applied to PA are given in Table 1. We analyze these data, with especially focusing on

Table 1. Comparison of Various Theoretical Approaches as Applied to PA

methodology	oligomer or band; A_x	BLA (Å)	E_g (eV)	ref
HF/STO-3G	band, $A_x = 1$	0.150		154g
HF/6-31G*	band, $A_x = 1$	0.137		154f
HF/6-31G*	band, $A_x = 1$	0.130	7.34	99
HF/p-dz	band, $A_x = 1$	0.117	6.61	166b
HF/ccpVTZ	band, $A_x = 1$	0.123		167b
LDA/9s5p(C)	band, $A_x = 0$	0.031	0.3	155c
LDA/6-31G*	band, $A_x = 0$	0.010	0.11	99
BLYP/6-31G*	oligomer, $A_x = 0$	0.015	0.14	77
BLYP/6-31G*	band, $A_x = 0$	0.018	0.17	99
BLYP/6-311G*	oligomer, $A_x = 0$	0.025	0.46	77
O3LYP/6-31G*	band, $A_x = 0.12$	0.040	0.70	99
B3LYP/6-31G*	oligomer, $A_x = 0.20$	0.051	1.10	119
B3LYP/6-31G*	oligomer, $A_x = 0.20$	0.048	1.00	77
B3LYP/6-31G*	band, $A_x = 0.20$	0.058	1.25	99
B3LYP/6-311G*	oligomer, $A_x = 0.20$	0.053	1.17	77
B3LYP/6-311G*	oligomer, $A_x = 0.20$	0.059		151
B3LYP/6-311G*	band, $A_x = 0.20$	0.057	1.24	99
B3P86-30%/CEP-31G*	oligomer, $A_x = 0.30$	0.064	1.57	163
BHandH	band, $A_x = 0.50$	0.084	3.19	99
KMLYP/6-31G*	band, $A_x = 0.557$	0.087	3.61	99
MP2/6-31G*	oligomer	0.050		162
MP2/6-311G*	oligomer	0.062		151
MP2/p-dz	band	0.082	2.75	166b
MP2/ccpVTZ	band	0.074		167b
UNO-CAS/6-31G*	oligomer	0.110		154f
CCSD/ccpVTZ	band	0.095		167b
CCSD(T)/ccpVTZ	band	0.086		167b
PW91PW91/plane wave	band, $A_x = 0$	0.024	0.21	168
DFT-LMTO	band, $A_x = 0$	0.061	2.7 ^a	160b
DFT-LMTO	band, $A_x = 0$	0.10	0.6	160a
experiment		0.08		76a
experiment		0.08		76b
experiment		0.09		76d
experiment		0.07		76c
experiment			1.48	78c

^a Estimated from Figure 21 of ref 161b.

the role of exact exchange content (value of A_x) on BLA and band gap.

We first note that the oligomer approach provides essentially the same information if extrapolated to infinity, as the k -space based band theory does. The geometry converges faster, because the frontier orbitals are more influenced by end effects than the geometry of the central repeat unit. Still, extrapolated values from oligomer calculations and values from band calculations do not exactly agree with one another. These differences are due to a number of factors, including lattice sum approximations in the band calculations and, naturally, on the other hand, the finiteness of the oligomers. Note that end effects may play important and counterintuitive roles, as will be discussed for systems with two valence tautomeric ground states, an aromatic and a quinonoid, in section 3.3. For the rest of the discussion, we turn to the role of the level of theory and nonlocal exchange. Generally, HF methods have the largest alternation, hybrid methods with A_x values around 50% are next, which are followed by coupled-cluster, singles and doubles (CCSD), MP2, and B3LYP (the latter has an A_x value close to 20%). Local density approximation (LDA) and BLYP (with $A_x = 0$) yield the smallest BLA and E_g . The agreement with experiment is best by CCSD, B3LYP, and MP2.

HF methods predict¹⁵⁴ a sizable BLA for PA. The calculated double bond is in the range of 1.32–1.37

Å, and the single bond is within 1.43–1.48 Å. The BLA values at HF level depend on the basis set, but all HF values are significantly larger than the experimental range,⁷⁶ which is around 0.07–0.09 Å. The calculated band gap based on Koopmans's theorem is unacceptable being several times larger than the experimental value.

Because of the limited performance of the HF, density functional methods have played a major role recently in the calculations on extended systems, which provide an affordable way of accounting for the important correlation effects at practically manageable computational costs. Mintmire and White¹⁵⁵ studied the dimerization problem of all-*trans*-PA within the LDA formalism employing the Gaspar–Kohn–Sham exchange–correlation potential. The BLA obtained is much smaller than the experimental value by roughly a factor of 3. Other LDA studies¹⁵⁶ also gave similar results: small bond alternation and a small band gap. The origin of this disagreement is associated with the well-known feature of LDA methods, which underestimate band gaps in insulators and semiconductors.¹⁵⁷ The introduction of gradient corrected (GGA) density functionals did not improve the performance of DFT in this respect significantly.¹⁵⁸ This may be linked to the treatment of nonlocality and asymptotic behavior by the existing density functionals leading to too small band gaps.¹⁵⁹ An exception may be the result of Springborg et al.,¹⁶⁰ who used a first-principle density functional LMTO (linearized muffin-tin orbital) method for PA. The exchange and correlation effects were treated by the local approximation of von Barth and Hedin.¹⁶¹ Through this method, they obtained reasonable alternation and band gap for PA. This method still needs further testing and validation to become more widely used.

These comparisons show that relative to the HF methods, local and gradient-corrected DFT overestimate the correlation effect without exact exchange mixing. A reasonable compromise is to use hybrid DFT schemes by mixing a certain empirically adjusted percentage (A_x) of exact HF exchange into the DFT exchange functionals. As discussed in connection with eq 16, this correction frequently leads to better agreement between theory and experiment. With one of the currently popular hybrid DFT functionals, B3LYP, Choi and Kertesz⁷⁷ showed that the BLA of PA obtained from the extrapolation of polyenes was 0.05 Å, in good agreement with MP2 calculations.¹⁶² Salzner and co-workers¹⁶³ used the Becke's three parameter hybrid density functional, with Perdew 86 nonlocal correlation functional (B3P86) formalism with $A_x = 30\%$ of exact exchange mixing to study PA by extrapolating polyene oligomer calculations. They showed that the central unit of a polyene with 24 carbon atoms has a double CC bond length of 1.380 Å and a single CC bond length of 1.444 Å, which are close to the experimental PA values of 1.36–1.39 and 1.44–1.46 Å, respectively. The extrapolated B3P86 band gap was 1.57 eV, very close to the experimental value of about 1.5 eV.⁷⁸ The BLA value from the B3 hybrid functional seems a little smaller, but the band gap value is accurate¹¹⁹

when experimental geometry is used in the calculation. This may be linked to the fact that the three parameters in the B3 scheme were determined by using atomization energies, ionization potentials, and other atomic energies.¹⁶⁴ Application to heteroaromatic systems shows that exact exchange mixing that is significantly larger than 30% leads to energy gaps that are too large.¹⁶⁵

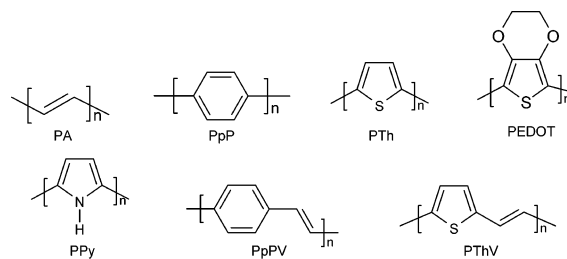
Many body perturbation theory (MBPT) in the second order (MP2) gives also a reasonable BLA value for PA.¹⁶⁶ As to the band gap, the MP2 value is still too large, but at least it is in the right order of magnitude. Going to the fourth order of perturbation theory, MP4 did not improve the results much further.¹⁶⁷ Yu^{167b} used coupled-cluster methods, CCSD, and CCSD(T), and also obtained satisfactory BLA values for PA, although they are not affordable for most systems.

It has been occasionally noted in the literature that the geometry optimization of a band calculation depends very sensitively on the number of k -points used to represent the BZ. This may not be surprising for complex three-dimensional (3D) metallic systems, where the question whether a particular k -point of a band is occupied or not may influence the results. However, this argument would not hold for PA or similar systems, such as polydiacetylenes (PDAs). Therefore, one would expect that for very simple band structures with a sizable band gap, such as PA or similar systems to be discussed in the next section, the number of k -points would affect the optimized geometry only slightly. It appears to us that in all cases when this problem has been observed, the level of theory was either LDA, GGA, or a similar theory without exact exchange contribution ($A_x \cong 0$). Therefore, the small band gaps, associated with such a situation, provide only a small driving force toward alternation that becomes sensitive to the sampling of the band in the vicinity of the gap. For instance, Sun et al.¹⁶⁸ observed that by increasing the k -point set from 20 to 100 k -points, the optimized bond alternation is reduced from 3.5 to 1.5 pm using a GGA form of DFT and a plane wave basis set. Moreover, the calculated alternation depends strongly on the smearing parameter, which is used to simulate nonzero temperature in band calculations. Some inconsistencies in the literature regarding the value of the alternation may be also related to the under-sampling of k -space in such LDA or LDA-like calculations. We think that one possible remedy is in using better density functionals with 20–30% exact exchange mixing leading to better overall results and better convergence properties with respect to k -space sampling, as indicated by the results on various polymers and annulenes discussed above.

3. Conjugated Polymers

A large number of conjugated polymers have been synthesized and studied in the last two decades. Their structures, electronic structures, and numerous properties have been reviewed extensively.¹⁶⁹ A few representative structural formulas are shown in **26**.

In addition to BLA, several other factors influence the band gaps of these complex systems. Most of the



26

factors involved are normally interdependent; no general formula can be given. For instance, as in the case of poly(thiophene), PTh, and poly(pyrrole), PPy, heteroatoms affect the gap by both influencing the degree of BLA and mixing of the heteroatom orbital. The latter can be viewed as a direct heteroatomic effect. For purely interpretative purposes, based on the perturbation approach of qualitative MO theory, the following qualitative formula expresses the main contributions affecting the band gap:¹⁷⁰

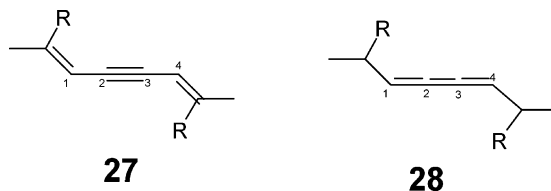
$$E_g \cong E_g^{\text{topol}} + E_g^{\Delta r} + E_g^{\theta} + E_g^{\text{arom}} + E_g^{\text{sub}} + E_g^{\text{error}} \quad (18)$$

where E_g^{topol} is the topological band gap, $E_g^{\Delta r}$ is the contribution from BLA or geometry relaxation along the main chain (including a large exchange contribution), E_g^{θ} is a contribution arising from the effect of ring torsion (nonplanarity), E_g^{arom} is owing to the presence of an aromatic ring along the chain, which limits π -electron delocalization outside the ring, E_g^{sub} comes from substitution effects, and E_g^{error} normally includes geometry defects, disorder, and interchain interactions. Bond distances play a key role in those cases, when the topological band gap is zero, e.g., PA or polyacene. However, the strong coupling of the frontier orbital(s) remains important even if the topological band gap is not zero, as is the case for all polymers in **26**, except PA. Therefore, the geometry influences the band gap directly.¹⁷¹ This is especially evident for polymers with two possible ground states, as will be discussed in the following sections.

3.1. PDA: A Prototype Conjugated Polymer with Two Nondegenerate Ground State Structures

First, we discuss the energetics and structures of a family of simple linear chain systems that are closely related to PA. These polymers are the PDAs, which can be represented in two alternative structures, the acetylenic (**27**) or A-PDA form, and the butatrienic (**28**) or B-PDA form. The alternation pattern is shifted in these two nondegenerate valence tautomers. This is in contrast to PA, where the two degenerate forms can be transformed into each other by shifting the alternation pattern from the even to the odd bonds or vice versa. Therefore, in the PDA case, there is no hypothetical equidistant form with a zero band gap; therefore, the concept of the Peierls distortion is not directly applicable. Polymers with this property constitute a large class of “nondegenerate ground state polymers”.¹⁷² We will discuss key results regarding PDA, which is the best-studied system in this class. The conclusions regarding PDA

will have important implications to other, practically more important nondegenerate ground state polymers, such as polythiophenes, polypyrroles, polyanilines, poly(*p*-phenylene)s, and their various copolymers with varying degrees of aromaticity.



A number of crystalline PDAs have been synthesized via topochemical polymerization allowing the determination of their structures by single crystal X-ray diffraction.¹⁷³ There are variations in the observed structures of the main carbon skeleton, but all observed structures correspond to the acetylenic (**27**) structure.¹⁷⁴ There is an obvious connection to the electronic structure of PA,¹⁷⁵ the main difference being that the two *sp* (rather than *sp*²) hybridized carbon atoms in each repeat unit create a locally different environment relative to their neighbors. This disruption of conjugation would create a nonzero band gap even if the Peierls distortion would not be operative. This built in difference with respect to PA also ensures a substantial energy difference between the two alternative forms. By mere inspection, one would likely find **27** to be the more stable form, because here the localized π -bonds between the two central *sp* carbon atoms in each cell are in phase with the bond alternation dictated by the Peierls distortion of the PA-like delocalized π -electron system. This is in agreement with what has been found experimentally and theoretically so far. Nevertheless, it is intriguing to explore this structural isomerism of the two alternative forms of PDA, because it shows similar features displayed by the structural isomerism of other conjugated polymers with more complex structures, such as PTh (**29**, **30**), polyisothianaphthene, PITN, (**31**, **32**), and many other thiophene, pyrrole, or furan based conjugated polymers and other systems. Compounds **29** and **31** are forms that can be called, for the sake of simplicity, the “aromatic” (A) form, while **30** and **32** can be called “quinonoid” (Q) forms. In reality, the actual geometries are usually between these two extremes, and in some circumstances, these extreme forms cannot be defined unequivocally. For instance, the structure and properties of poly(*para*-phenylene), PpP, or poly(*p*-phenylenevinylene), PpPV (**26**), can be discussed in these terms¹⁷⁶ even though the quinonoid valence tautomeric forms in these two cases are high energy structures. Figure 13 shows the schematic behavior of the PES along the generalized reaction coordinate connecting the two forms of PA (degenerate case) and PpP (nondegenerate case). There are local excitations in which the structures of the repeat units resemble those of the higher energy structure. An example of such a “polaron” would be a few rings with Q structure for polythiophene plus a few rings with intermediate structures so that the excitation represents a localized deviation from the otherwise

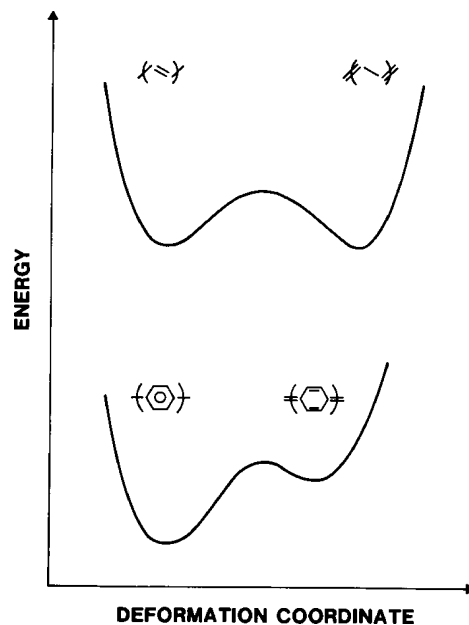
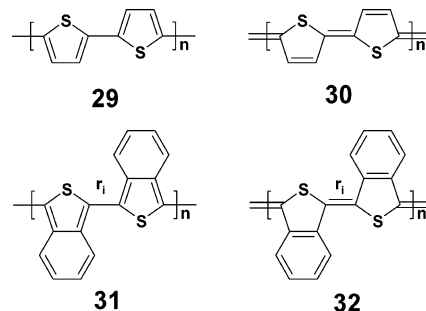


Figure 13. Schematic potential energy curve along the reaction coordinate connecting two forms of a conjugated polymer. Top: PA, degenerate case; bottom: PpP, nondegenerate case. Reprinted with permission from ref 172. Copyright 1986 Marcel Dekker, Inc.

aromatic (A type) polymer. These types of local excitations, which can be created by optical means or by doping (charge transfer), are very important in interpreting a number of properties of the undoped (pristine and nonconducting phases) as well as the highly doped (conducting phases) conducting polymers.^{177,178}



Several investigators emphasized the strong coupling between the generalized reaction coordinate, connecting these two idealized structures, and the energy levels of the frontier orbitals.^{179,180} This “electron–phonon” coupling is strong, essentially linear, and somewhat analogous to the case of PA, as expressed by eq 2. The generalized reaction coordinate in question connects the A and Q forms (or the A-PDA and the B-PDA forms in case of PDA), and it primarily involves the change of the BLA along the carbon skeleton of the long polymer backbone chain and is related to a level crossing of the HO and LU pair of orbitals.¹⁸¹ We shall denote this coordinate as q_{AB} for PDA and q_{AQ} for the aromatic–quinonoid pairs, as in **29** and **30**. This coordinate can be approximated by a linear path, assuming that the

Table 2. Theoretical and Experimental CC Bond Distances and Band Gap of the Acetylene Form of PDA (A-PDA, 27)^a

methodology	r_{12} (Å)	r_{23} (Å)	$r_{41'}$ (Å)	BLA (Å)	E_g (eV)	ref
HF/7s3p/3s	1.42	1.19	1.32	0.17		182
HF/6-31G	1.424	1.200	1.337	0.156	7.68	185
HF/6-31G*	1.430	1.193	1.331	0.168	8.00	185
MP2/6-31G	1.41	1.23	1.37	0.11		151
MP2/6-31G//HF/6-31G*	1.430	1.193	1.331	0.168	5.89	185
MP2/6-311G	1.42	1.23	1.37	0.12		188
BHandH/6-31G*	1.399	1.207	1.344	0.124	3.67	99
B3LYP/6-31G	1.403	1.228	1.371	0.104	1.72	185
B3LYP/6-31G*	1.401	1.224	1.368	0.105	1.68	185
PBE/plane wave	1.39	1.23	1.38	0.09		191
BLYP/6-31G*	1.395	1.240	1.392	0.079	0.55	99
experiment	1.43	1.19	1.36	0.16		174a
experiment	1.43	1.18	1.37	0.16		174b
experiment	1.44	1.21	1.33	0.17		174c
experiment	1.41	1.21	1.36	0.13		174d
experiment	1.43	1.19	1.36	0.16	2.0	174e

^a The BLA is defined as $\delta = r_{12} - (r_{23} + r_{41'})/2$, where the labels refer to the numbering in **27**.

coordinates of the A form are q_A and those of the Q form are q_Q :

$$q_{AQ} = q_A + a(q_Q - q_A) \quad (19)$$

The analogy with PA is apparent (q_{AQ} reduces to q_{BLA} for PA), but the key difference is that the two structures associated with q_A and q_Q are not degenerate, leading to a different band gap behavior.

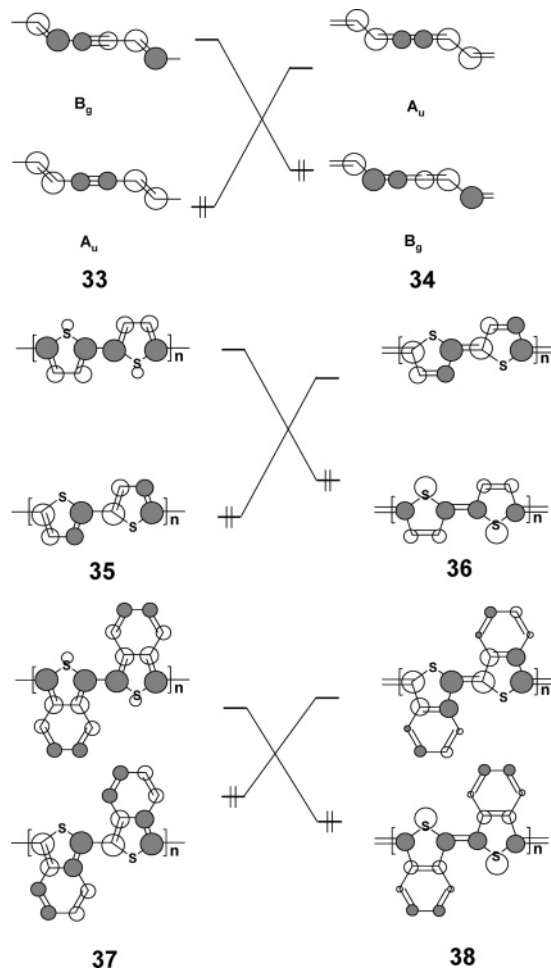
Karpfen¹⁸² has shown that the two alternative structures of PDA can be connected with each other via such a simple linear generalized coordinate that transforms all triple and single bonds in A-PDA into double bonds and all double bonds in A-PDA into single bonds. Karpfen used hydrogen atoms to represent the side groups in his early HF CO calculations and found a small barrier close to the higher energy (butatrienic) form. The acetylenic form is found to be significantly more stable than the butatrienic form in other studies as well.¹⁸³ This transition, moving from the acetylenic form (**27**) to the butatrienic form (**28**), connects the frontier orbitals of the two valence tautomers through a level crossing, as shown in **33** and **34**, leading to an energy barrier on the PES along the q_{AQ} reaction coordinate. The level crossing¹⁸² can be understood entirely by focusing on the PA like pattern of all four π -orbitals represented in **33** and **34**. A very similar level crossing occurs for the A-Q pair of PTh (**35** and **36**) and PITN (**37** and **38**), which will be discussed in detail in the next section. Representative calculated optimized geometries and band gaps for A-PDA are collected in Table 2 and compared with experiments. Bond alternation values correlate with the percent exact exchange content, although less clearly as in the case of PA, due to the localized bonding provided by the π_v -orbitals of the central sp-sp bonds. The alternation values and the corresponding band gaps follow similar trends as for PA. It is worth noting that the experimental uncertainties of the bond distances are rather large for these systems for a variety of reasons, as discussed by Enkelman, including various influences of side groups, imperfect polymerization,

Table 3. Theoretical Geometry and Band Gap of the Butatriene Form of PDA (B-PDA, 28)^a

methodology	r_{12} (Å)	r_{23} (Å)	$r_{41'}$ (Å)	BLA (Å)	E_g (eV)	ref
HF/STO-3G	1.32	1.24	1.46	-0.03		182
HF/7s3p/3s	1.32	1.25	1.44	-0.03		182
HF/3-21G	1.314	1.249	1.451	-0.030		185
HF/6-31G	1.322	1.256	1.449	-0.031		185
HF/6-31G*	1.317	1.255	1.453	-0.037		185
MP2/6-31G	1.38	1.25	1.42	0.05		151
MP2/6-311G	1.34	1.27	1.48	-0.035		188
BHandH/6-31G*	1.332	1.244	1.416	0.002	1.71	99

^a The BLA is defined as $\delta = r_{12} - (r_{23} + r_{41'})/2$, where the labels refer to the numbering in structure **28**.

and lack of anisotropic thermal vibrational corrections for the bond distances.¹⁸⁴



The alternation pattern of the bond distances in **33** stabilizes the A_u orbital and destabilizes the B_g orbital in a similar manner as the two degenerate nonbonding π -orbitals are split by the Peierls distortion in PA as shown in Figure 9. The roles are not entirely reversed in **34**, because the middle (triple) bond becomes longer than but not as long as a single bond. Consequently, the band gap of B-PDA is much smaller than in A-PDA, as shown in Table 3, and its total energy is correspondingly higher.

Tobita et al.¹⁸⁵ have extensively explored the PES of the A- to B-PDA transition. They also reviewed the theoretical literature on PDAs before 2001. They used

a number of methods including HF, B3LYP, and MP2 with different basis sets. Their main conclusion confirmed the earlier HF results of Karpfen insofar as two minima were found at the HF level. However, Tobita et al. noted that at higher levels of the theory, only A-PDA is a true minimum on the PES when using MP2 or B3LYP. They also obtained satisfactory agreement between the calculated and the observed¹⁸⁶ vibrational frequencies. However, the agreement is not sufficiently close to serve as a basis of fully confirming the structural predictions.

Suhai¹⁸⁷ has used correlation methods and exciton theory to describe the electronic excitations in PDA. Tobita et al. also addressed the issues of excited states and band gaps. They concluded that the hybrid DFT (specifically the B3LYP functional) provides much better band gap values than HF or MP2.^{187,188} Table 2 compares a few calculated band gap values together with experimental ones. The nature of the exciton binding energy remains an interesting problem for PDA and other conjugated polymers, but its discussion would lead too far from the main subject of this review.¹⁸⁹ Other properties, such as polarizabilities, are of great interest but remain also challenging to calculate for PDA and similar polymers.¹⁹⁰

Recent detailed calculations reinforced the conclusion that A-PDA is much more stable than B-PDA by using several alternative density functionals.¹⁹¹ The key observation from this study was that the PES has a very small barrier close to the higher energy butatrienic form, in agreement with Hammond's principle. The second minimum is very sensitive to the level of theory and does not appear as a minimum for most, such as B3LYP, in agreement with the findings of Tobita et al.¹⁸⁵ The presence or absence of the second minimum is also sensitive to the number of *k*-points in the BZ sampling, which is a disturbing feature indicating that this is a rather subtle feature on the PES. The situation is somewhat reminiscent to the critical n_{cr} value discussed in the "transition" from alternating to nonalternating ground states for $[4n + 2]$ annulenes in section 2.3. Either a higher level of theory or a particularly well-parametrized DFT would be needed, which would likely produce very accurate bond alternation, band gap, and ultimately accurate energy values for the two forms of PDA.

In contrast to earlier studies,¹⁹² Katagiri et al. found that side groups might have a noticeable effect on the band gaps and PES.¹⁹¹ This issue is relevant in searching for new forms of PDA with tunable properties. Because of the level crossing associated with the transition between the two forms, the band gap is sensitive to the location of the minima. The closer the structure to the level crossing, the smaller the expected band gap may become. Thus, a form of band gap engineering may become possible, by utilizing side groups, cross-links, and ladder type topologies. This will be explored in the next section before turning to heteroconjugated polymers.

3.2. Ladder Polymers and Networks Built from Polyenes and PDAs

On the basis of the principles developed above, one should be able to analyze and predict the properties

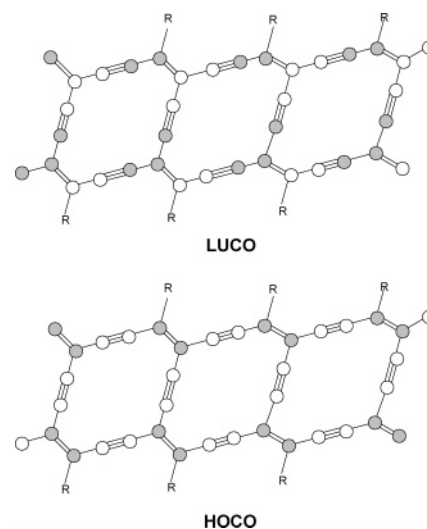
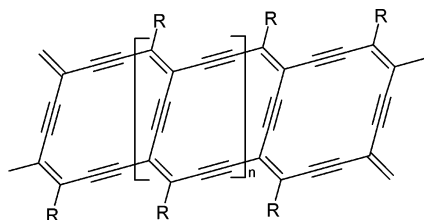
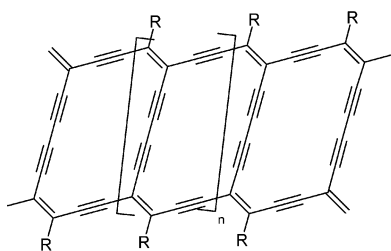


Figure 14. Two frontier orbitals, HOCO and LUCO, of the ACPDAL (**39**). R's refer to substituents.

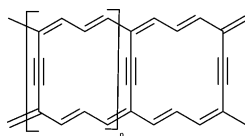
of more complex ladder structures and 2D,¹⁹³ even 3D, networks that maintain a high level of conjugation.¹⁹⁴ Because of the large number of possibilities, many networks can be imagined; there is much work to be done.¹⁹⁵

PDA chains are synthesized through repeated 1,4-additions of substituted diacetylenes in a solid state polymerization process.¹⁷³ When oligoynes with different sizes or longer oligoynes are used as monomers in the polymerization, PDA ladders, or even 2D, 3D diacetylene networks, may be formed. A typical structure of such a ladder, an acetylene coupled poly-substituted-diacetylenic ladder (ACPDAL) is illustrated in **39**. The acetylenic steps of the "ladder" can be replaced by longer oligoyne units with the formula $-(C\equiv C-)_s-$.¹⁹⁶ Structure **39** corresponds to the $s = 1$ case. The PDA chains may be coupled every one, two, or more diacetylene units along two "rails" of the ladder. When $s = 2$, the system can be called a diacetylene coupled polydiacetylene ladder (DACPDAL, **40**), which is the only one that has been obtained experimentally so far.¹⁹⁷ This system has also been extensively studied by a series of spectroscopic techniques.^{198–200} The properties of the ladder can be further tuned by substitutions at the side group R. Generally, one would expect that the couplings through the oligoyne units add extra conjugation pathways for these ladder polymers, relative to the parent pair of PDAs.⁸² This coupling would be qualitatively different from the case of polyacene, as discussed before, because in that case the frontier orbitals are localized on the edge carbons. However, in this case, the interchain interaction between the two PDA "rails" of the ladder mediated by the oligoyne "steps" of the ladder lead to a significant splitting of both the highest valence band and the lowest conduction band of the PDA single chain. As a result of the splitting, one expects that the band gap of the ladder system will be reduced as compared to the PDA chain. This can also be seen from a qualitative CO analysis as shown in Figure 14. The HOCO level of the ladder system is raised due to the in phase interaction between the two orbitals on the PDA "rails", which is communicated

through the acetylene linking “steps”. Similarly, the LUCO level of the ladder system is reduced, due to an out of phase interaction. Therefore, the band gap of the ladder system is reduced substantially. With PBC calculations at the B3LYP/6-31G* level, the band gap of ACPDAL, **39**, is reduced significantly to 0.68 eV,²⁰¹ as compared to 1.68 eV, the gap of the PDA single chain when calculated at the same level.¹⁸⁵ The further change from **39** ($s = 1$) to the next member of the series with $s = 2$ (DACPDAL, **40**), is modest, giving a band gap of 0.79 eV. Longer linking steps (larger s) give rise to less coupling and therefore less gap reduction relative to the PDA backbone reference system.

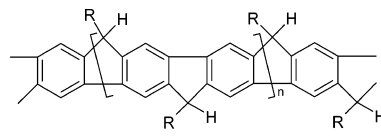
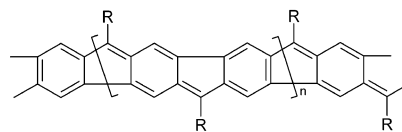
**39****40**

When the PDA chains are replaced by PA chains, a new class of ladder systems can be imagined. The steps of the ladder will remain oligoynes rather than oligoynes, because of steric effects in the case of the latter. The simplest member is **41**. A dimerlike unit has been characterized by X-ray single crystal diffraction, showing two oligoene “rails” connected by three “steps” of a molecule that can be thought of as the beginning of a ladder.²⁰² A trend similar to the one observed for the PDA ladders is expected. The band gap of acetylene coupled polyacetylene ladder (ACPAL, **41**) is reduced to about 0.4 eV, as compared with 1.25 eV for PA single chain, with both values calculated from the PBC calculation at the B3LYP/6-31G* level.²⁰¹

**41**

Several different forms of low band gap ladder polymers have been studied. Planarized poly-*p*-phenylenes (PLPpP, **42**) are important, as they represent a more complete π -delocalization than the nonplanarized version, PpP (**26**). Their properties have been reviewed by Scherf,²⁰³ together with the electronically

more interesting ladder type poly(arylenemethine) polymers, **43**. These latter systems display a Peierls type distortion due to the seventh (odd) π -electron in the chemical repeat unit, leading to an alternation of the aromatic and quinonoid structures along the chain.¹⁸⁰ (The repeat unit formula for polymer **43** shows two such units with 14 π -electrons after the Peierls distortion has been taken into account. Technically, the method of “band backfolding” relates the energy bands of the doubled unit cell with those of the smaller unit cell with a screw axis of symmetry.²⁰⁴) The calculated LHS band gap is small as compared to that of PA, between 0.7 and 0.9 eV, while the bandwidth is still sufficiently large to allow for charge carrier delocalization along the polymer chain. The agreement with experiment is reasonable.²⁰⁵ Recent calculations on derivatives of these systems focused on the control of the gap by using side groups.²⁰⁶ Interesting, but experimentally yet unconfirmed, predictions of magnetism in these polymers stem from a very narrow band near the Fermi level obtained in the calculation.

**42****43**

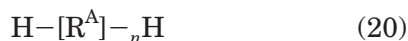
There is much work that is underway in various laboratories. Successes of the synthetic strategies of Diederich at al.¹⁹⁵ indicate that more ladder and other 2D π -aromatic systems are becoming viable. A resurgence in the synthesis of dehydrobenzoannulenes opened opportunities for making new annulene networks.²⁰⁷ In the next two sections, we will turn to another family of polymers that exhibit two non-degenerate ground states. First, we discuss some general trends based on oligomer considerations.

3.3. Oligomer Size Dependencies of Conjugated Heteroaromatics

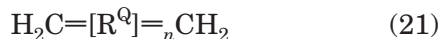
As discussed in the case of PDA, the calculated relative stability of A-PDA vs B-PDA depends on the level of theory. The same is true for other polymers (**26**) with two different ground states, such as PTH and PITN.

An oligomer-based method has been developed to deal with this problem, based on the proposition that the ground state of an oligomer can be switched from, say the aromatic (A) form to the quinonoid (Q) form by replacing a singly bonded terminal $-H$ (or $-CH_3$) group by another terminal group connected to the last repeat unit by a double bond, say $=CH_2$ at both ends of the oligomer. This substitution switches the alternation pattern from A to Q, e.g., from **29** to **30**, as shown in **44** and **45**. A similar “forcing” of the A or Q structures by terminal groups is shown in **46** and **47**

for the PITN polymer (**31** and **32**). By varying the number of chemical repeat units, n , between the two kinds of terminations, one arrives at two series of oligomer molecules:



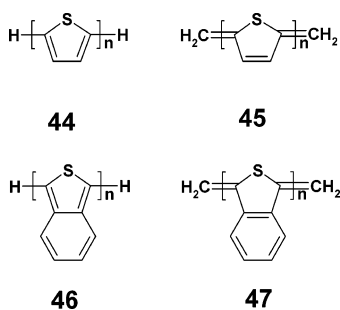
and



where R^{A} and R^{Q} represent the two valence tautomeric structures of the very same chemical repeat unit R. Their respective energies, at any given level of theory, are $E^{\text{A}}(n)$ and $E^{\text{Q}}(n)$. Assuming that the oligomer approaches the polymer with increasing size, the incremental change of the energy after the virtual insertion of the next repeat unit yields a per repeat unit (pru) energy for both series:

$$E_{\text{pru}}^{\text{A}}(n) = E^{\text{A}}(n) - E^{\text{A}}(n-1) \text{ and } E_{\text{pru}}^{\text{Q}}(n) = E^{\text{Q}}(n) - E^{\text{Q}}(n-1) \quad (22)$$

If n is sufficiently large, this $E_{\text{pru}}(n)$ value should



be the same as obtained by PBC total energy calculations. Actually, this fact can be exploited for testing periodic computer codes. Fast convergence of variants of this method as a function of n has been noted in many cases.²⁰⁸ This method can be used to establish which of the two alternative forms are more stable by calculating the difference series:

$$E_{\text{pru}}^{\text{AQ}}(n) = E^{\text{A}}(n) - E^{\text{Q}}(n) \quad (23)$$

The method relies on the difference (eq 23) of differences (eq 22). Applications of this method²⁰⁹ have helped to confirm the preference of the A form for PTh, PpP, and PPY and the Q form for PITN, in agreement with MNDO level band theory total energy calculations.¹⁷⁰ The oligomer method not only informs which of the two is more stable but it also gives an estimate for the relative pru energies as defined in eq 23.

The orbital interpretation of the stability change from the A to the Q form is straightforward using PBC and is given in **35** and **36** for PTh and in **37** and **38** for PITN. Note that by comparing the A forms (**35** and **37**) one notices a relative destabilization due to the fused rings in each chemical repeat unit, while the opposite trend occurs for the Q forms (**36** and **38**). This trend can be extended to further fused rings, such as in poly(isonaphthothiophene), etc.²¹⁰ Accordingly, the perturbative effects of the fused aromatic

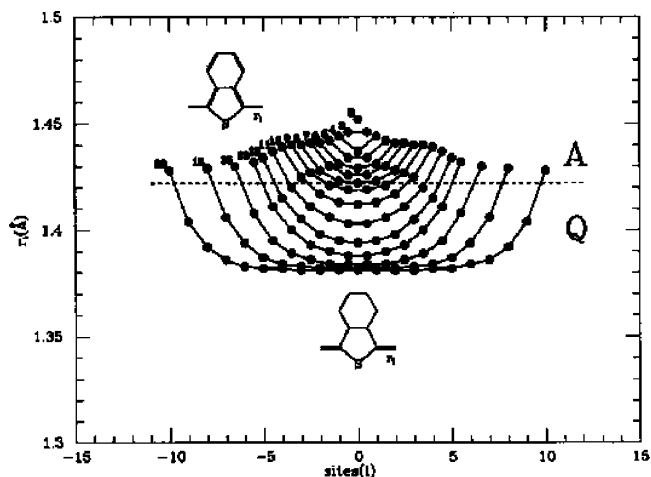


Figure 15. Variation of optimum bond lengths (r_i) along ITN oligomers with different numbers of monomers (n). The value of n is indicated by bold face numerals. Solid lines are used to connect dots representing bond lengths of a given oligomer. The dashed line separates the regions that can be called aromatic (A) and quinonoid (Q). Reprinted with permission from ref 212. Copyright 1990 American Physical Society.

rings stabilize the quinonoid form of the thiophene unit. Further calculations and experiments confirmed this switchover, although ambiguity remains because the experimentally made oligomers and polymers are not terminated by double bonds, as would be required to have a uniform quinonoid structure throughout the whole PITN chain.²¹¹

This problem can be best understood by the insightful model calculations by Kürti and Surjan.²¹² They have done a series of oligomer calculations on PITN but used a termination that is not a double but a single bond ($-\text{H}$). Thus, for short oligomers, the structure is clearly aromatic (**46**). However, as the length of the oligomer is increased in the calculation, the geometry in the middle segment begins to deviate from the aromatic bond pattern and starts to resemble that of the quinonoid form as can be seen in Figure 15, where the interring bond lengths, r_i , are used to characterize the aromatic or quinonoid nature of the two repeat units adjacent to the i -th bond. As n increases, the development of the quinonoid type structure in the center is clearly recognizable, and beyond $n = 10$ or so units, the geometry of the middle segment starts to converge. The two end groups remain aromatic with a smooth transition toward the middle quinonoid units. These calculations show the limitations of the oligomer method in obtaining an estimate for the pru energy difference, $E_{\text{pru}}^{\text{AQ}}(n)$, showing that the estimate will depend on n . Nevertheless, the oligomer approach provides direct information on the preferred structure or tautomeric form. Furthermore, the middle segment can be used, if sufficiently large, for structural predictions for the infinite chain.

A note on the level of theory is in order. The marked structural differences between the middle segment and the end groups emerge only for oligomers with several unit cells, and thus, this type of calculation requires relatively large resources if they are done at higher levels of theory. Kürti and Surjan

used a form of the LHS Hamiltonian. It includes only a distance-dependent π -electron Hückel term and a distance-dependent restoring force due to σ -electrons. A better known version of essentially the same model is the Su–Schrieffer–Heeger Hamiltonian.²¹³ Both are capable of describing the alternation and the gap if properly parametrized.

The oligomer method has also been used frequently in obtaining extrapolations for properties of polymers other than stability or total energy, most commonly for the band gap, E_g . The method often relies on an asymptotics, such as

$$E_{\text{HOMO-LUMO}}(n) \approx E_g + \text{const}/n + \dots$$

where the oligomer HOMO–LUMO gap approaches the band gap of the infinite chain. However, deviations from this size dependency have often been observed.^{91,211,214,215} The difficulty of the oligomer method can be appreciated by referring to Figure 15. As the chain length is increased, the central part of the system resembles the polymer more and more. However, a mixture of aromatic, quinonoid, and intermediate repeat units, each with its unique contribution toward the frontier and other orbitals, generally leads to a rather complex behavior as a function of $1/n$.

3.4. Aromatic vs Quinonoid Structures of Conjugated Polymers

Several investigators have used the oligomer approach to obtain the geometry of the polymer repeat unit by focusing on the central units of large oligomers and then using these as the starting point of energy band calculations based on that geometry without further geometry optimization. This process provides reliable results for the ground state.

There have been a number of applications of these ideas to heteroconjugated polymers.²¹⁶ Oligomers of various sizes are used, applying standard quantum chemical techniques such as AM1, MNDO, or even B3LYP, often followed by a band calculation using either a tight binding method, such as extended Hückel,^{175,217} or a DFT method.^{119,163,218} A recent study by Tachibana et al.²¹⁹ shows how the aromatic vs quinonoid competition, discussed in section 3.3, can be efficiently dealt with in oligomer calculations with large repeat units. In this representative calculation, first the geometry of large oligomers is optimized with MO methods. If the oligomers are sufficiently long, the middle segments are assumed to be characteristic of the polymer repeat unit. This is then followed by extended Hückel band calculations in order to obtain the energy bands of the polymer. Tachibana et al. applied B3LYP level oligomer calculations for the smaller models and used PM3 for the larger ones due to computer time limitations. Overall, this mixed strategy seems to work well and provides sufficient accuracy for interpreting the experimental results for various aromatic, quinonoid, and mixed polymers. As mentioned in connection with PA, the oligomer and the band (PBC) methods converge to each other and are often used separately or in combination.

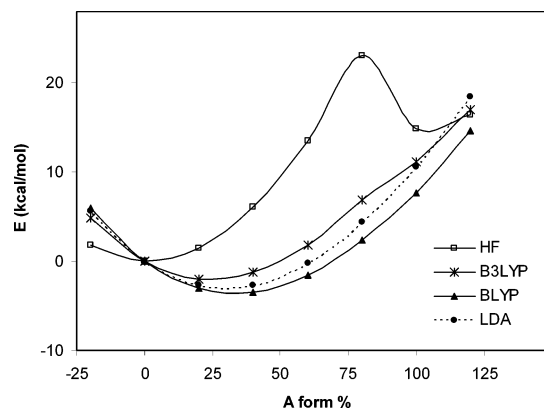


Figure 16. Total energy curves of polythiophene along the linear reaction coordinate connecting the two minima (A and Q), obtained by four different theoretical methods. A and Q are determined from HF potential surface. a is the % quinonoid character, representing a linear reaction coordinate defined in eq 19. The 6-31G* basis set was used with PBC calculations.

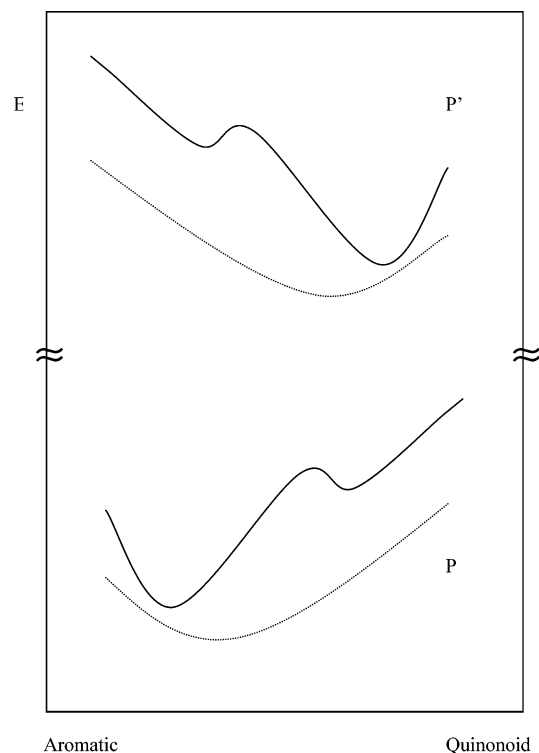

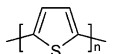
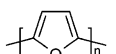
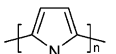
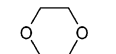


Figure 17. Schematic PES of an unsubstituted polymer with repeat unit P and substituted polymer with repeat unit P'. The horizontal axis corresponds to a generalized coordinate (q) connecting the aromatic form (A) with the quinonoid form (Q). Continuous lines indicate the PES at one level of theory where both minima exist for both P and P', while at some other level of theory, indicated by the dashed lines, only one minimum is present.

This mixed approach yields results that on the one hand help interpret the experimentally available band gap values and can also be used for exploratory predictions. Tables 4 and 5 give a small selection of experimental²²⁰ and predicted band gaps obtained by the oligomer or band methods.^{210,221,165} Data in Table 4 refer to primarily aromatic structures, while those in Table 5 refer to quinonoid ones. The existence of aromatic rings in the monomer usually enlarges the band gap of the corresponding polymers relative to

Table 4. Typical Aromatic (A) Conjugated Polymers and Their Band Gaps (in eV)

entry	structure	theory			experiment	
		methodology	E_g	ref	E_g	ref
48		B3LYP/6-31G*/PM3, oligomer	2.81	119		
		B3LYP/6-31G*, band	3.08	99		
		Hückel//MNDO, band	2.74	170	3.0	220a
		EHT//MNDO, band	3.44	217a		
		VEH, band//MNDO, oligomer	2.90	217b		
29		B3LYP/6-31G*/PM3, oligomer	1.90	119		
		B3LYP/6-31G*, band	2.05	99		
		EHT, Band // PM3, oligomer	2.05	219		
		TD-B3LYP/6-31G*, oligomer	1.60	216	2.1-2.2	220b
		ZINDO//B3LYP/6-31G*, oligomer	1.78	216		
		Hückel//MNDO, band	1.83	227		
		B3P86-30%/CEP-31G*, oligomer	2.30	163		
		B3LYP/6-31G*, band	2.42	99		
		B3LYP/6-31G*/PM3, oligomer	2.13	165	2.4	220d
49		EHT//PRDDO, band	2.93	217a		
		B3P86-30%/CEP-31G*, oligomer	2.67	163		
		B3LYP/6-31G*/PM3, oligomer	2.38	119		
		B3LYP/6-31G*, band	2.88	99		
50		Hückel//MNDO, band	2.95	227	2.8	220c
		EHT//MNDO, band	3.18	217a		
		B3P86-30%/CEP-31G*, oligomer	3.16	163		
		B3LYP/6-31G*/PM3, oligomer	2.38	119		
51		B3LYP/6-31G*, oligomer	1.61	165		
		B3LYP/6-31G*, band	1.83	99	1.6-1.7	220f
		B3P86-30%/CEP-31G*, oligomer	2.06	218		
		DFT/plane wave, band	1.04	221b		

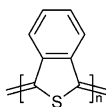
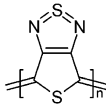
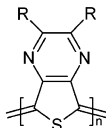
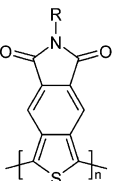
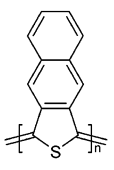
PA as can be seen from the data in Table 4. On the other hand, some quinonoid polymers have band gaps, smaller than that of PA. At this point, no simple intuitive procedure exists that can provide similarly reliable results. It appears that only high level calculations can answer the question whether the aromatic or quinonoid structure is the ground state and then provide further electronic structure information, such as the band gap.

The preference of an aromatic or quinonoid ground state is related to the presence or absence of the second minimum on the PES of the systems listed in Tables 4 and 5 and similar conjugated polymers and copolymers. A key issue is how and under which circumstances chemical modifications can switch the relative stability of the A and the Q forms.

As discussed in connection with the example of A-PDA and B-PDA, the existence of one or two local

minima on the PES is dependent on the model chemistry employed. Figure 16 shows the 1D PES of polythiophene calculated by four different methods.¹⁶⁵ Only the HF method shows two local minima; these were chosen as the A and Q structures. The geometry was a linear reaction coordinate along the two minima (A and Q) of the HF potential surface. Parameter a is the % quinonoid character, which is a linear reaction coordinate defined in eq 19. The 6-31G* basis set was used with PBCs. The results are in many respects similar to the ones discussed for PDA. On the basis of the analysis of band gaps and bond alternation in this review, it seems highly likely that the second minimum is either very shallow or does not even exist. On the other hand, the single minimum structure contains a significant percent of quinonoid character for the B3LYP method (relative to HF) that appears as most reliable among the four

Table 5. Typical Q Form Conjugated Polymers with Their Band Gaps (in eV)

entry	structure	theory			experiment	
		methodology	E_g	ref	E_g	ref
32		B3LYP/6-31G*, oligomer	1.29	165	1.0	220h
		B3LYP/6-31G*, band	1.44	99		
		Hückel//MNDO, band	1.16	170		
		VEH, Band//MNDO, oligomer	0.54	179b		
		PITN	B3LYP/6-31G*, oligomer	0.47		
		DFT/plane wave, band	0.54	221b		
52		B3LYP/6-31G*, band	2.18	99		
		HF/STO-3G, band	9.13	221a		
		DFT/plane wave, band	0.83	221b		
53		B3LYP/6-31G*, band	1.32	99	0.95	220i
		B3LYP/6-31G*, oligomer	0.47	216		
		ZINDO//B3LYP/6-31G*, oligomer	0.49	216		
		EHT, band//PRDDO, oligomer	0.70	217c		
54		B3LYP/6-31G*, band	1.10	99	1.2	220j
55		Hückel//MNDO, band	1.50	210	1.5	220k
		EHT, band//PRDDO, oligomer	1.10	217c		
		B3LYP/6-31G*, band	1.93	99		
	PNIT					

methods studied here. The shift of the minimum toward the other structure (toward Q in the case of A and vice versa) is an indication of the important role that electron correlation plays as discussed in the Introduction and in section 2.

The presence or absence of the second minimum has important implications. Let us discuss the general case, as illustrated in Figure 17, for the polymer P and its modified variant, P'. (The example could be PTh, **29** and **30**, and PITN, **31** and **32**.) If both local minima are maintained during the modification from P to P', the discussion can refer to stabilizing or destabilizing structures A or Q relative to one another. However, if the local minima of the less stable structures do not appear on the PES, it is still useful to maintain the conceptual framework of the four structures allowing qualitative discussions of the perturbing effects that stabilize the previously higher energy structure. The example of PTh (A) to PITN (Q) illustrates such a situation, even though in many calculations neither PTh(Q) nor PITN (A) appear as local minima.

Aromatic rings in the monomer usually enlarge the band gap of the corresponding polymers relative to

PA. On the other hand, some of the quinonoid systems also have large band gaps. In the following discussion, we put these seemingly contradictory trends in the context of the PES as illustrated in Figure 17. First, among aromatic polymers, the gap increase comes from a competition between π -electron confinement within the rings and delocalization along the chain.²²² Therefore, it is expected that for these polymers the band gaps can be reduced by increasing the quinonoid character of the polymer backbone.^{179,209} For PpP, PTh, and PPy, aromatic forms are more stable at the ground state, but the corresponding quinonoid structures have much smaller band gaps. As discussed above, in many cases, a quinonoid structure cannot be identified on the PES as a local minimum. Nevertheless, the modification of the structure toward the quinonoid structure in these cases amounts to moving closer to the level crossing, and therefore, it results in a reduction of the gap. On the other hand, PITN²²³ and other polymers have a quinonoid ground state. (See also Table 5.) In an isothianaphthene, ITN unit, a competition exists between the aromaticity of a benzene ring and that of a thiophene ring. Because the former has a larger

resonance energy than the latter, an ITN unit takes the geometry of a combination of an aromatic benzene ring and a quinonoid thiophene ring (Q form). The more stable Q form of PITN has a relatively larger band gap than the A form but a much smaller band gap when compared to the parent polymer of PTh. Various strategies toward band gap design that build on these general considerations will be discussed in the next section.

3.5. Controlling the Band Gap of Conjugated Polymers through Change of Aromaticity

A number of publications have dealt with the control of designing polymeric materials with desired electronic properties, low band gaps, or band gaps matching required values.^{14,224} We round out this review by focusing on two types of small band gap polymers that utilize the aromatic–quinonoid transition and hinge upon the essential connection between bond distances and frontier electronic energy levels. A different approach for designing conjugated polymers with desired electronic structures is based on alternating donor and acceptor units, which do not fall within the purview of this work.²²⁵

The concept of the A–Q transition has been in the background of much of the efforts in designing low band gap conjugated polymers. The most representative example is the reduction of the band gap from PTh (A form, 2.1–2.2 eV) to PITN (Q form, 1.0 eV), by incorporating quinonoid character into the system.^{179b} As mentioned in the previous section, neither A nor Q character in a conjugated system in itself insures a small band gap. The effect of A and Q characters on the band gap may be mostly taken through the BLA (δ) change. Suppose two minima, A and Q, exist along the BLA coordinate. In our convention, $\delta(A)$ is negative and $\delta(Q)$ is positive placing the aromatic structure to the left, as in Figures 13 and 17 on the PES. It is the absolute value of δ in a real system that directly affects the band gap, not the sign. Most conjugated polymers, like PpP, Ppy, and PTh, occur in the aromatic geometry in their undoped ground states, thus, increasing the quinonoid character of the conjugated system at the expense of its aromatic character, which will reduce the band gap. For some conjugated polymers as listed in Table 5, the more stable form is the Q form. To reduce the band gap for these systems, the aromatic character should be increased if gap reduction is the goal. Increasing the quinonoid character actually increases the band gap instead of decreasing it, as can be seen in Table 6.

How does one achieve the modification of the aromatic or quinonoid character of the polymer backbone? Various strategies have been explored; we mention two typical approaches. The first is to use methineline connections in the following manner.²²⁶ This construction uses the chemical repeat unit of



where R may be a phenyl or thiophene unit. By linking the R units by a CH unit that has an odd number of π -electrons, one can anticipate a half-filled

Table 6. Band Gaps of Polythiophene and Its Derivatives with Additional Fused Rings, Based on the MNDO Geometry Optimization Followed by Hückel Theory Band Calculation^a

entry	29	32	55	56
systems				
aromatic	1.83	0.73	0.28	0.08
quinonoid	0.47	1.16	1.50	1.66

^a The values corresponding to the more stable valence tautomeric forms are in bold.²¹⁰

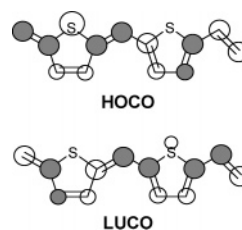


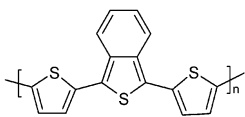
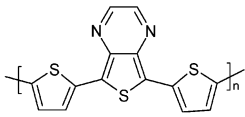
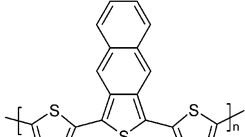
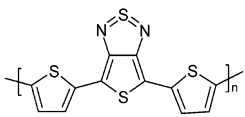
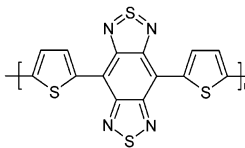
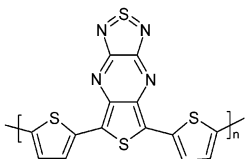
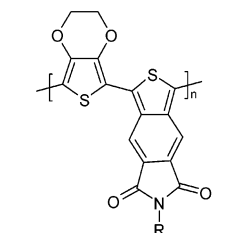
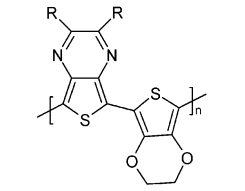
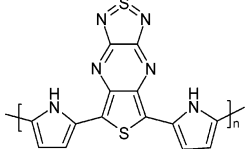
Figure 18. Schematic orbital patterns of the frontier COs of a methine-linked polythiophene polymer. One unit cell composed of two chemical repeat units plus one atom from each of the neighboring cells is shown; the orbitals correspond to $k = 0$.

band situation and a Peierls distortion leading to a unit cell doubling:



An example of this idea is illustrated in Figure 18, where the relevant HOCO and LUCO orbitals are shown.²²⁷ The geometry of the two adjacent thiophene (R) units displays A and Q characters in an alternating fashion, and the gap is reduced. It is tempting to attribute the reduction of the gap relative to that of thiophene to the presence of the quinonoid-like thiophene units. However, an alternative interpretation that can be generalized is that the frontier orbitals are very similar to those of PA (insert in Figure 9). Deviations from the frontier orbitals of the PA “backbone” (the mixing of the sulfur π -orbitals of every second thiophene unit) explain the gap reduction relative to that of PA. One concludes that this approach can reduce the gap substantially. However, in all methine coupling examples, there will be a nonzero gap due to the half-filled band nature of the system (the methine unit provides an odd π -electron per chemical repeat unit), making it susceptible to Peierls distortion, similar to the ladder type poly(arylenemethine)s, **43**. Further studies extended this connection to various heteroaromatic methine-linked polymers.^{224,228} Recently, this idea was extended to the poly(3,4-ethylenedioxythiophene) (PEDOT, **26**) repeat unit resulting in a large gap reduction to about 0.9–1.0 eV and displaying an alternation of quinonoid and aromatic structures.²²⁹ Note that PEDOT is

Table 7. Band Gaps (in eV) of Some Experimentally Available A–Q Copolymers

entry	structure	theory			experiment	
		methodology	E_g	ref	E_g	ref
57		LHS, band	1.29	232	1.7±0.1	231a
		B3LYP/6-31G*, band	1.32	99		
58		B3LYP/6-31G*, band	1.21	99	1.0	231d
59		LHS, band	0.88	232	0.65	231e
60		B3LYP/6-31G*, band	0.59	99	0.90	231g
		HF/STO-3G, band	5.97	221a		
61		B3LYP/6-31G*, band	0.98	99	<0.5	231h
62		EHT, band//PM3,oligomer	0.47	219	<0.5	231i
63		B3LYP/6-31G*, band	1.02	99	1.0	231j
64		B3LYP/6-31G*, band	0.79	99	0.36	231k
65		EHT, band//PM3,oligomer	0.33	219	0	231l

another low gap fused ring polythiophene derivative, which was first developed by scientists at the Bayer AG research laboratories in Germany, and has developed into one of the most successfully conjugated polymers in practical application.²³⁰

The second approach is copolymerization of A and Q units. The idea is that the chemically different units have an intrinsically aromatic character (e.g., thiophene, Th), while the others display an intrinsically quinonoid character (e.g., isothianaphthene,

ITN). In the copolymer, then, the connecting bonds will be “pushed” away from their stable “intrinsic” structures, toward a level crossing leading to a reduced gap. This motif can be varied, leading to poly(–Th –ITN–) or poly(–Th –ITN –Th–). More generally, these copolymers can be described as poly($A_n Q_m$). (The order within the unit cell matters and various ordered and disordered polymers can be envisioned.) Poly(AQ) has the disadvantage of being possibly disordered, leading to narrow bands even if the gap might be small. Note that A and Q in this case represent different chemical entities. The strategy leads to gap reduction relative to the gaps of the respective polymer with the repeat unit of A [poly(A)] and poly(Q) homopolymers.

In such an A–Q copolymer, the overall BLA δ of the whole polymer, if it can be defined, is the average of the alternation of the subunits $\delta(A)$ and $\delta(Q)$, which may be different in absolute values but opposite in sign. [Note that $\delta(A)$ and $\delta(Q)$ are not the same as the corresponding values in poly(A) and poly(Q).] Therefore, the absolute value of δ is smaller than both $\delta(A)$ and $\delta(Q)$ as the result of the mixing, leading to an effectively reduced bond alternation and band gap. Copolymers using any A unit similar to those listed in Table 4 and any Q unit similar to those in Table 5 and a large number of derivatives and combinations may be pursued. Some experimental results²³¹ are listed in Table 7 for reference, together with a few theoretical predictions.^{165,219,221a,232} Intuitively, the lowest band gap copolymers are obtained when the strength of the aromatic character of an A unit and that of the quinonoid character of a Q unit are about the same; in other words, $\delta(A)$ and $\delta(Q)$ due to their opposite signs can practically cancel. Heteroatom effects, fused rings, and other factors such as nonplanarity still contribute toward increasing the gap. Nevertheless, intrinsic conducting polymers with close to zero band gaps and with significant bandwidths, allowing high conductivity, may be achievable.

Comparing the results in Table 7 with Tables 4 and 5, it is apparent that band gaps are lowered significantly for most A–Q copolymers relative to the poly(A) and poly(Q) homopolymers. Some of these copolymers do not show a significant gap reduction experimentally probably due to a combination of finite size effects, nonplanarity, and impurities. The design of single strand conjugated polymers with an intrinsic band gap of 0.1–0.2 eV remains a compelling challenge.^{14,233,234}

4. Summary and Outlook

We have reviewed the effect of system size on aromaticity via the geometric bond alternation parameter, δ , and the energy gap associated with this distortion from uniform bond distances. The distortive nature of the π -electron JT effect drives the bond alternation for both open shell and closed shell systems. Although it is still not clear when it happens, as the system size increases, a structural transition from a delocalized to a localized valence tautomeric form occurs in the series of $[4n + 2]$ -annulenes, which are considered Hückel aromatic

molecules. This transition demonstrates the distortive nature of π -electrons in conjugated system and bridges the practical and conceptual gap between the finite and extended systems. The expansion from one to two dimensions, however, shows a diminishing distortive tendency of the bond distances and a reduction of the associated band gap eventually leading to very small band gaps in “metallic” single wall carbon nanotubes and the well-known zero band gap for graphene. On the other hand, bond alternation plays apparently a smaller role in *s*-indacene, which is a $4n$ annulene with two transannular bonds.

Numerous calculations for linear chain aromatic and conjugated polymers are reviewed with particular emphasis on the role of nonlocal exchange, which enhances both bond alternation and band gap. Oligomer methods for polymer calculations are reviewed, and the reasons for slow convergence for some systems with two valence tautomeric forms are analyzed.

The geometries and electronic structures of heteroconjugated polymers with two valence tautomeric ground states are reviewed. These include PDAs (acetylenic vs butatrienic forms) and polythiophene-based polymers (aromatic vs quinonoid forms) and their analogues. The role of bond alternation and its effect on properties is emphasized. Ladder polymers based on PDA are discussed.

Design principles for small band gap conjugated polymers are reviewed. The role of bond alternation with respect to structure and gap is emphasized. Aspects of band gap engineering and the critical evaluation of widely used computational methods for polymer properties are also discussed. It is pointed out that intrinsic conducting polymers with close to zero band gaps and with significant bandwidths may be achievable.

5. Notations and Abbreviations

A_x	Exact exchange factor in hybrid DFT
a	Linear reaction coordinate in AQ transition
ACPAL	Acetylene coupled polyacetylenic ladder
ACPDAL	Acetylene coupled polydiacetylenic ladder
AM1	Austin model 1
AQ	Aromatic to quinonoid [transition]
ASE	Aromatic stabilization energy
B1	Becke's one parameter hybrid density functional
BLYP	Becke exchange with Lee, Yang, Parr correlation functional
B3LYP	Becke's three parameter hybrid density functional, with Lee–Yang–Parr nonlocal correlation functional
B3PW91	Becke's three parameter hybrid density functional, with Perdew–Wang 91 nonlocal correlation functional
B3P86	Becke's three parameter hybrid density functional, with Perdew 86 nonlocal correlation functional
BHandH	Becke's half and half functional, with Slater local exchange, and Lee–Yang–Parr nonlocal correlation functional
BHandHLYP	Becke's half and half functional, with Becke 88 nonlocal exchange, and Lee–Yang–Parr nonlocal correlation functional
BLA	Bond length alternation

BZ	Brillouin zone
CASPT2	Complete active space, second-order perturbation theory
CASSCF	Complete active space self-consistent field
CCSD	Coupled-cluster, singles and doubles
CCSD(T)	Coupled-cluster, singles and doubles with approximate triples
CI	Configuration interaction
CNDO/S	Complete neglect of differential overlap/spectroscopic parametrization
CO	Crystal orbital
δ	Bond length alternation
1D, 2D, 3D	One-, two-, and three-dimensional
DACPDAL	Diacetylene coupled polydiacetylenic ladder
DBMP	1,3-Di- <i>tert</i> -butyl-4,5-dimethyl-carboxypentalene
DFT	Density functional theory
DOS	Density of states
E_g	Energy band gap
E_i	i -th orbital energy
$E_i(k)$	i -th energy band
EHT	Extended Hückel theory
GGA	Generalized gradient-corrected approximation
HF	Hartree–Fock
HOMAS	Harmonic oscillator model of aromatic stability
HOO	Highest occupied (molecular or crystal) orbital
HOSE	Harmonic oscillator stabilization energy
JT	Jahn–Teller
KMLYP	Kang–Musgrave hybrid density functional
LDA	Local density approximation
LDA-BP	Density functional with Becke 88 nonlocal exchange and Perdew 86 nonlocal correlation functional
LHS	Longuet–Higgins and Salem
LMTO	Linearized muffin-tin orbital
LUO	Lowest unoccupied (molecular or crystal) orbital
MBPT	Many body perturbation theory
MCSCF	Multiconfiguration self-consistent field
MNDO	Modified neglect of diatomic overlap
MNDOC	Electron correlated modified neglect of diatomic overlap
MO	Molecular orbital
MP2	Møller–Plesset second-order perturbation theory
N	number of π -electrons
n_{cr}	Critical n value for $[4n + 2]$ annulenes
PA	Polyacetylene
PBC	Periodic boundary condition
PDA	Polydiacetylene
PES	Potential energy surface
PEDOT	Poly(3,4-ethylenedioxythiophene)
PITN	Polyisothianaphthene
Poly(A)	Polymer with the repeat unit of A
PLPpP	Planarized poly(<i>para</i> -phenylene)
PM3	Modified neglect of diatomic overlap-parametrization method 3
PpP	Poly(<i>para</i> -phenylene)
PPP	Pariser–Parr–Pople
PPy	Poly(pyrrole)
PTh	Poly(thiophene)
pru	Per repeat unit
q	Reaction coordinate
qAQ	Reaction coordinate connecting the aromatic–quinonoid structures
SWCN	Single wall carbon nanotube
TDDFT	Time-dependent density functional theory
TTBP	1,3,5-Tri- <i>tert</i> -butylpentalene

TZP	Triple- ζ polarized basis sets
UHF	Unrestricted Hartree–Fock
ZDO	Zero differential overlap
ZINDO	Zerner's version of the intermediate neglect of differential overlap

6. Acknowledgments

Research at Georgetown University has been supported by the NSF Grant DMR-0331710 and research at Kyungpook National University has been supported by Korea Research Foundation (Grant KRF-2002-005-C00009). We are indebted to Prof. Y. Gartstein for insightful discussions on carbon nanotubes.

7. References

- (1) (a) Lloyd, D. M. G. *Carbocyclic Non-Benzenoid Aromatic Compounds*; Elsevier: Amsterdam, 1966. (b) *Non-Benzenoid Aromatics*; Snyder, J. P., Ed.; Academic Press: New York, 1969; Vol. 1. (c) *Non-Benzenoid Aromatics*; Snyder, J. P., Ed.; Academic Press: New York, 1971; Vol. 2. (d) Labarre, J. P.; Crasnier, F. *Top. Curr. Chem.* **1971**, *24*, 33. (e) Haddon, R. C.; Haddon, V. R.; Jackman, L. M. *Top. Curr. Chem.* **1971**, *16*, 2. (f) *Aromaticity, Pseudo-Aromaticity, Anti-aromaticity*; Bergmann, E. D., Pullman, B., Eds.; Jerusalem Symposium on Quantum Chemistry and Biochemistry; Israel Academy of Science and Humanities: Israel, 1971; Vol. 3. (g) Mallion, R. B. *Pure Appl. Chem.* **1980**, *52*, 1541. (h) Lloyd, D. M. G. *Nonbenzenoid Conjugated Carbocyclic Compounds*; Elsevier: Amsterdam, 1984. (i) Garratt, P. J. *Aromaticity*; Wiley: New York, 1986. (j) Balaban, A. T.; Banciu, M.; Ciorba, V. *Annulenes, Benzo-, Hetero-, Homo-Derivatives, and Their Valence Isomers*; CRC Press: Boca Raton, Florida, 1987; Vol. I–III. (k) Lloyd, D. *The Chemistry of Conjugated Cyclic Compounds: To Be or Not To Be Like Benzene?* John Wiley & Sons: New York, 1989. (l) Sainsbury, M. *Aromatic Chemistry*; Oxford University Press: Oxford, 1992. (m) Minkin, V. J.; Glukhovtsev, M. N.; Simkin, B. Y. *Aromaticity and Antiaromaticity; Electronic and Structural Aspects*; Wiley: New York, 1994.
- (2) von Schleyer, P. R., Ed. *Chem. Rev.* **2001**, *101* (5).
- (3) For a recent review, see Krygowski, T. M.; Cyrański, M. K. *Chem. Rev.* **2001**, *101*, 1385 in ref 2.
- (4) Longuet-Higgins, H. C.; Salem, L. *Proc. R. Soc. London* **1959**, *A251*, 172.
- (5) Ovchinnikov, A. A.; Ukrainskii, I. I.; Kventsel, G. F. *Usp. Fiz. Nauk.* **1972**, *108*, 81.
- (6) (a) Julg, A.; Francois, P. *Theor. Chem. Acta* **1967**, *7*, 363. (b) Julg, A. *A New Definition of the Degree of Aromaticity in Aromaticity and Pseudo-Aromaticity*; The Israel Academy of Sciences and Humanities: Jerusalem, 1971.
- (7) (a) Kruszewski, J.; Krygowski, T. M. *Tetrahedron Lett.* **1972**, 3839. (b) Krygowski, T. M. *J. Chem. Inf. Comput. Sci.* **1993**, *33*, 70.
- (8) (a) Bird, C. W. *Tetrahedron* **1985**, *41*, 1409. (b) Bird, C. W. *Tetrahedron* **1986**, *42*, 89. (c) Bird, C. W. *Tetrahedron* **1992**, *48*, 335.
- (9) Krygowski, T. M.; Wieckowski, T. *Croat. Chem. Acta* **1981**, *54*, 193.
- (10) (a) Binsch, G.; Heilbronner, E.; Murrell, J. N. *Mol. Phys.* **1966**, *11*, 305. (b) Binsch, G.; Heilbronner, E. *Tetrahedron* **1968**, *24*, 1215. (c) Binsch, G.; Tamir, I.; Hill, R. D. *J. Am. Chem. Soc.* **1969**, *91*, 2446. (d) Binsch, G.; Tamir, I. *J. Am. Chem. Soc.* **1969**, *91*, 2450. (e) Nakajima, T. *Top. Curr. Chem.* **1972**, *32*, 1. (f) Toyota, A.; Nakajima, T. *Bull. Chem. Soc. Jpn.* **1977**, *50*, 97. (g) Toyota, A.; Nakajima, T.; Koseki, S. *J. Chem. Soc., Perkin Trans. 2* **1984**, 85. (h) Nakajima, T.; Toyota, A.; Kataoka, M. *J. Am. Chem. Soc.* **1982**, *104*, 5610.
- (11) See, for example, Cyrański, M.; Krygowski, T. M.; Katritzky, A. R.; von Schleyer, P. R. *J. Org. Chem.* **2002**, *67*, 1333.
- (12) Chiang, C. K.; Fincher, C. R.; Park, Y. W.; Heeger, A. J.; Shirakawa, H.; Louis, E. *J. Phys. Rev. Lett.* **1977**, *39*, 1098.
- (13) (a) *Handbook of Conducting Polymers*; Skotheim, T. A., Ed.; Dekker: New York, 1986; Vols. 1 and 2. (b) *Conjugated Polymeric Materials*; Bredas, J. L., Chance, R. R., Eds.; Kluwer Academic: Dordrecht, 1990. (c) *Conjugated Polymers*; Bredas, J. L., Silbey, R., Eds.; Kluwer Academic: Dordrecht, 1991. (d) *Conjugated Conducting Polymers*; Kiess, H. G., Ed.; Springer-Verlag: Berlin, 1992. (e) *Conjugated Polymers and Related Materials*; Salaneck, W. R., Lundstrom, I., Ranby, B., Eds.; Oxford University Press: New York, 1993.
- (14) Leading references are as follows: (a) Roncali, J. *Chem. Rev.* **1997**, *97*, 173. (b) Pomerantz, M. In *Handbook of Conducting*

- Polymers*, 2nd ed.; Skotheim, T. A., Elsenbaumer, R. L., Reynolds, J. R., Eds.; Dekker: New York, 1998; p 277.
- (15) (a) Su, W. P.; Schrieffer, J. R.; Heeger, A. J. *Phys. Rev. Lett.* **1979**, *42*, 1698. (b) Rice, M. J. *Phys. Lett.* **1979**, *A71*, 1521.
- (16) Horowitz, B.; Vardeny, Z.; Ehrenfreund, E.; Brafman, U. *Synth. Met.* **1984**, *9*, 215.
- (17) See, for example, Zerbi, G.; Gussoni, M.; Castiglioni, C. In *Conjugated Polymers*; Bredas, J. L., Silbey, R., Eds.; Kluwer Academic: Dordrecht, 1991.
- (18) Peierls, R. *Quantum Theory of Solids*; Oxford University Press: New York, 1955; p 108.
- (19) See Soos, Z. G.; Mukhopadhyay, D.; Painelli, A.; Girlando, A. In *Handbook of Conducting Polymers*, 2nd ed.; Skotheim, T. A., Elsenbaumer, R. L., Reynolds, J. R., Eds.; Dekker: New York, 1998; p 165.
- (20) (a) Coulson, C. A. *Nature* **1947**, *159*, 265. (b) Coulson, C. A.; Taylor, R. *Proc. Phys. Soc. A* **1952**, *65*, 815.
- (21) Koutecky, J.; Zahradnik, R. *Collect. Czech. Chem. Comm.* **1960**, *25*, 811.
- (22) (a) Ladik, J.; Appel, K. *J. Chem. Phys.* **1964**, *40*, 2470. (b) Ladik, J. *Calculation of the Electronic Structure of Organic Polymers as Solids*; Plenum: New York, 1988.
- (23) Popov, N. A.; Shustorovich, E. M. *Zh. Strukturnoi Khim.* **1965**, *6*, 286.
- (24) Andre, J. M. *J. Chem. Phys.* **1969**, *50*, 1536.
- (25) Whangbo, M.-H.; Hoffmann, R. *J. Am. Chem. Soc.* **1978**, *100*, 6093.
- (26) Any list would have to be incomplete, since many research groups have custom-made programs. The programs widely used are as follows: YAEHMOP, MOSOL (Mopac), CAESAR, CRYSTAL, ADF, ACES, and Gaussian 03. For current information on these packages, see Google.
- (27) See, for example, Sun, G. Y.; Kürti, J.; Rajczy, P.; Kertesz, M.; Hafner, J.; Kresse, G. *J. Mol. Struct.: THEOCHEM* **2003**, *624*, 37.
- (28) See, for instance, (a) Hoffmann, R. *Solids and Surfaces: A Chemist's View of Bonding in Extended Structures*; VCH: New York, 1988. (b) *Quantum Mechanical Ab Initio Calculation of the Properties of Crystalline Materials*; Pisani, C., Ed.; Springer: Berlin, 1996.
- (29) *The Irreducible Representations of Space Groups*; Zak, J., Ed.; W. A. Benjamin: New York, 1969.
- (30) Saito, R.; Fujita, M.; Dresselhaus, G.; Dresselhaus, M. S. *Phys. Rev. B* **1992**, *46*, 1804.
- (31) Kertesz, M.; Vonderviszt, F.; Hoffmann, R. In *Intercalated Graphites*; Dresselhaus, M. S., Dresselhaus, G., Fisher, J. E., Moran, M. J., Eds.; Elsevier: New York, 1983; p 141.
- (32) (a) Jahn, H. A.; Teller, E. *Proc. R. Soc. (London)* **1937**, *A161*, 220. (b) Ham, F. S. *Int. J. Quantum Chem. Symp.* **1971**, *5*, 191. (c) Marenich, A. V.; Boggs, J. E. *J. Phys. Chem. A* **2004**, *108*, 10594.
- (33) (a) Irgartinger, H.; Rodewald, H. *Angew. Chem., Int. Ed. Engl.* **1974**, *13*, 740. (b) Delbaere, L. R. J.; James, M. N. G.; Nakamura, N.; Masamune, S. *J. Am. Chem. Soc.* **1975**, *97*, 1973. (c) Irgartinger, H.; Riegler, N.; Malsch, K.-D.; Schneider, K.-A.; Maier, G. *Angew. Chem., Int. Ed. Engl.* **1980**, *19*, 211. (d) Borden, W. T.; Davidson, E. R. *J. Am. Chem. Soc.* **1980**, *102*, 7958. (e) Irgartinger, H.; Nixdorf, M. *Angew. Chem., Int. Ed. Engl.* **1983**, *22*, 403.
- (34) Dunitz, J. D.; Krüger, C.; Irgartinger, H.; Maverick, M. F.; Wang, Y.; Nixdorf, M. *Angew. Chem., Int. Ed. Engl.* **1988**, *27*, 387.
- (35) Degeneracy in this context refers to two distinct but energetically equivalent minima on the PES, which are valence tautomers, not to electronic degeneracy.
- (36) Albright, T. A.; Burdett, J. K.; Whangbo, M.-H. *Orbital Interactions in Chemistry*; Wiley: New York, 1985.
- (37) (a) Sunberg, K. R.; Ruedenberg, K. In *Quantum Science*; Calais, J. L., Goscinski, O., Linderberg, J., Öhrn, Y., Eds.; Plenum: New York, 1976. (b) Cheung, L. M.; Sunberg, K. R.; Ruedenberg, K. *Int. J. Quantum Chem.* **1979**, *16*, 1103. (c) Ruedenberg, K.; Schmidt, M.; Gilbert, M. M.; Elbert, T. S. *Chem. Phys.* **1982**, *71*, 41. (d) Roos, B. O.; Taylor, P.; Siegbahn, P. E. *Chem. Phys.* **1980**, *48*, 157. (e) Schmidt, M. W.; Gordon, M. S. *Annu. Rev. Phys. Chem.* **1998**, *49*, 233.
- (38) Koseki, S.; Toyota, A. *J. Phys. Chem. A* **1997**, *101*, 5712.
- (39) (a) Dewar, M. J. S.; Gleicher, G. J. *J. Am. Chem. Soc.* **1965**, *87* (4), 685. (b) Libkowitz, K. B.; Larter, R. *Tetrahedron Lett.* **1978**, *1*, 33. (c) Voter, A. F.; Goddard, W. A., III. *J. Am. Chem. Soc.* **1986**, *108*, 2830. (d) Martin, C. H.; Freed, K. F. *J. Chem. Phys.* **1996**, *105*, 1437. (e) Dijkstra, F.; Van Lenthe, J. H.; Havenith, R. W. A.; Jenneskens, L. W. *Int. J. Quantum Chem.* **2003**, *91*, 566.
- (40) Balci, M.; McKee, M. L.; Schleyer, P. v. R. *J. Phys. Chem. A* **2000**, *104*, 1246.
- (41) Herzberg, G. *Molecular Spectra and Molecular Structure: Infrared and Raman Spectra of Polyatomic Molecules*, reprint ed.; Krieger Pub. Co.: 1991; p 362.
- (42) Ermer, O. *Angew. Chem., Int. Ed. Engl.* **1987**, *26*, 782.
- (43) (a) Almlöf, J.; Faegri, K. *J. Chem. Phys.* **1983**, *79*, 2284. (b) Haddon, R. C.; Raghavachari, K. *J. Am. Chem. Soc.* **1985**, *107*, 289. (c) Ozkabak, A. G.; Goodman, L.; Wiberg, K. B. *J. Chem. Phys.* **1990**, *92*, 4115. (d) Handy, N. C.; Maslen, P. E.; Atoms, R. D.; Murray, C. W.; Laming, G. *J. Chem. Phys. Lett.* **1992**, *197*, 506.
- (44) Berry, R. S. *J. Chem. Phys.* **1961**, *35*, 2253.
- (45) Shaik, S. S.; Bar, R. *Nouv. J. Chim.* **1984**, *8*, 411.
- (46) (a) Shaik, S.; Hiberty, P. C. *J. Am. Chem. Soc.* **1985**, *107*, 3089. (b) Shaik, S. S.; Hiberty, P. C.; Ohanessian, G.; Lefour, J. M. *J. Org. Chem.* **1986**, *51*, 3908. (c) Shaik, S. S.; Hiberty, P. C.; Lefour, J. M.; Ohanessian, G. *J. Am. Chem. Soc.* **1987**, *109*, 363. (d) Shaik, S. S.; Hiberty, P. C.; Ohanessian, G.; Lefour, J. M. *J. Phys. Chem.* **1988**, *92*, 5086. (e) Ohanessian, G.; Hiberty, P. C.; Lefour, J. M.; Flament, J. P.; Shaik, S. S. *Inorg. Chem.* **1988**, *27*, 2219. (f) Hiberty, P. C. *Top. Curr. Chem.* **1990**, *153*, 27. (g) Hiberty, P. C.; Shaik, S. *Chem. Phys. Chem.* **2004**, *6*, 224.
- (47) Jug, K.; Köster, A. *J. Am. Chem. Soc.* **1990**, *112*, 6772.
- (48) Glending, E. D.; Faust, R.; Streitwieser, A.; Vollhardt, K. P. C.; Weinhold, F. *J. Am. Chem. Soc.* **1993**, *115*, 10952.
- (49) Hiberty, P. C.; Danovich, D.; Shurki, A.; Shaik, S. *J. Am. Chem. Soc.* **1995**, *117*, 7760.
- (50) Haas, Y.; Zilberg, S. *J. Am. Chem. Soc.* **1995**, *117*, 5387.
- (51) (a) Shaik, S.; Shurki, A.; Danovich, D.; Hiberty, P. C. *J. Am. Chem. Soc.* **1996**, *118*, 666. (b) Shaik, S.; Shurki, A.; Danovich, S.; Hiberty, P. C. *J. Mol. Struct. (THEOCHEM)* **1997**, *398–399*, 155.
- (52) Ma, B.; Sulzbach, H. M.; Remington, R. B.; Schaefer, H. F., III. *J. Am. Chem. Soc.* **1995**, *117*, 8392.
- (53) Subramanian, G.; Schleyer, P. v. R.; Jiao, H. *Angew. Chem., Int. Ed. Engl.* **1996**, *35*, 2638.
- (54) Epiotis, N. D. *Deciphering the Chemical Code*; VCH Publishers: New York, 1996.
- (55) Yu, Z.; Xuan, Z.; Wang, T.; Yu, H. *J. Phys. Chem.* **2000**, *104*, 1736.
- (56) Choi, C. H.; Kertesz, M.; Jiao, H.; Schleyer, P. v. R. (2002–2004, in preparation for publication).
- (57) Craig, D. P.; Maccoll, A. *J. Chem. Soc.* **1949**, *11*, 964.
- (58) (a) Chung, A. L. H.; Dewar, M. J. S. *J. Chem. Phys.* **1965**, *42*, 756. (b) Dewar, M. J. S.; de Llano, C. *J. Am. Chem. Soc.* **1969**, *91*, 789. (c) Hess, B. A.; Schaad, L. J. *J. Am. Chem. Soc.* **1971**, *93*, 305. (d) Baird, N. C.; West, R. M. *J. Am. Chem. Soc.* **1971**, *93*, 3072.
- (59) Kitzschke, B.; Lindner, H. *J. Tetrahedron Lett.* **1977**, *29*, 2511.
- (60) Falchi, A.; Gellini, C.; Salvi, P. R.; Hafner, K. *J. Phys. Chem.* **1995**, *99*, 14659.
- (61) (a) Hafner, K.; Suess, H. U. *Angew. Chem.* **1973**, *85*, 626. (b) Volz, H.; Kowarsch, H. *Heterocycles* **1977**, *7*, 1319.
- (62) Hafner, K.; Stowasser, B.; Krimmer, H.-P.; Fisher, S.; Böhm, M. C.; Lindner, H. *J. Angew. Chem., Int. Ed. Engl.* **1986**, *25*, 630.
- (63) Dunitz, J. D.; Krüger, C.; Irgartinger, H.; Maverick, E. F.; Wang, Y.; Nixdorf, M. *Angew. Chem., Int. Ed. Engl.* **1988**, *27*, 387.
- (64) The chemistry literature widely uses the terms localized vs delocalized as synonymous pairs with the terms symmetrical vs bond alternating, respectively.
- (65) Balaban, T. S.; Schardt, S.; Sturm, V.; Hafner, K. *Angew. Chem., Int. Ed. Engl.* **1995**, *34*, 330.
- (66) (a) Hertwig, R. H.; Holthausen, M. C.; Koch, W.; Maksic, Z. B. *Angew. Chem., Int. Ed. Engl.* **1994**, *33*, 1192. (b) Hertwig, R. H.; Holthausen, M. C.; Koch, W.; Maksic, Z. B. *Int. J. Quantum Chem.* **1995**, *54*, 147.
- (67) Gellini, C.; Cardini, G.; Salvi, P. R.; Marconi, G.; Hafner, K. *J. Phys. Chem.* **1993**, *97*, 1286.
- (68) Gellini, C.; Angeloni, L.; Salvi, P. R.; Marconi, G. *J. Phys. Chem.* **1995**, *99*, 85.
- (69) (a) Nakajima, T.; Saijo, T.; Yamaguchi, H. *Tetrahedron* **1964**, *20*, 2119. (b) Binsch, G.; Heilbronner, E.; Murrell, J. N. *Mol. Phys.* **1966**, *11*, 305.
- (70) Heilbronner, E.; Yang, Z. *Angew. Chem., Int. Ed. Engl.* **1987**, *26*, 360.
- (71) Nendel, M.; Goldfuss, B.; Houk, K. N.; Hafner, H. *J. Mol. Struct. (THEOCHEM)* **1999**, *461–462*, 23.
- (72) Nendel, M.; Houk, K. N.; Tolbert, L. M.; Vogel, E.; Jiao, H.; Schleyer, P. v. R. *J. Phys. Chem. A* **1998**, *102*, 7191.
- (73) Jartin, R. S.; Ligabue, A.; Soncini, A.; Lazzeretti, P. *J. Phys. Chem. A* **2002**, *106*, 11806.
- (74) Salem, L. *Molecular Orbital Theory of Conjugated Systems*; Benjamin: New York, 1966.
- (75) (a) Kertesz, M. *Adv. Quantum Chem.* **1982**, *15*, 161. (b) Ladik, J. J. *Quantum Theory of Polymers and Solids*; Plenum Press: New York, 1988. (c) André, J. M.; Delhalle, J.; Bredas, J. L. *Quantum Chemistry Aided Design of Organic Polymers*; World Scientific: Singapore, 1991. (d) Karpfen, A. In *Polydiacetylenes*; Bloor, D.; Chance, R. R., Eds.; NATO ASI Series E. V102; Nijhoff: Dordrecht, 1985.
- (76) (a) Fincher, C. R., Jr.; Chem, C.-E.; Heeger, A. J.; MacDiarmid, A. G. *Phys. Rev. Lett.* **1982**, *48*, 100. (b) Yannoni, C. S.; Clarke, T. C. *Phys. Rev. Lett.* **1983**, *51*, 1191. (c) Duijvestijn, M. J.;

- Manenshijn, A.; Schmidt, J.; Wind, R. A. *J. Magn. Reson.* **1985**, *64*, 451. (d) Kahlert, H.; Leitner, O.; Leising, G. *Synth. Met.* **1987**, *17*, 467. (e) Zhu, Q.; Fisher, J. E. *Solid State Commun.* **1992**, *83*, 179.
- (77) Choi, C. H.; Kertesz, M.; Karpfen, A. *J. Chem. Phys.* **1997**, *107*, 6712.
- (78) (b) Etemad, S.; Baker, G. L.; Roxlo, C. B.; Weinberger, B. R.; Orenstein, J. *Mol. Cryst. Liq. Cryst.* **1985**, *117*, 275. (c) Tani, T.; Grant, P. M.; Gill, W. D.; Street, G. B.; Clarke, T. C. *Solid State Commun.* **1980**, *33*, 499.
- (79) (a) Kertesz, M.; Surján, P. R. *Solid State Commun.* **1981**, *39*, 611. (b) Boudreaux, D. S.; Chance, R. R.; Frommer, J. E.; Bredas, J. L.; Silbey, R. *Phys. Rev. B* **1985**, *31*, 652.
- (80) Salem, L.; Longuet-Higgins, H. C. *Proc. R. Soc. (London)* **1960**, *A255*, 435.
- (81) Kertesz, M.; Hoffmann, R. *Solid State Commun.* **1983**, *47*, 7236.
- (82) Burdett, J. K. *Chemical Bonding in Solids*; Oxford: New York, 1995; p 62.
- (83) Houk, K. N.; Lee, P. S.; Nendel, M. *J. Org. Chem.* **2001**, *66*, 5517.
- (84) Gyulmaliev, A. M. *Zh. Fiz. Chim.* **1986**, *60*, 1682.
- (85) Čížek, J.; Paldus, J. *J. Chem. Phys.* **1970**, *53*, 821.
- (86) (a) Tanaka, K.; Ohzeki, K.; Nankai, S.; Yamabe, T.; Shirakawa, H. *J. Phys. Chem. Solids* **1983**, *44*, 1069. (b) Kertesz, M.; Lee, Y. S.; Stewart, J. J. P. *Int. J. Quantum Chem.* **1989**, *35*, 305.
- (87) Raghun, C.; Pati, Y. A.; Ramasesha, S. *Phys. Rev. B* **2002**, *65*, 155204.
- (88) Choi, H. S.; Kim, K. S. *Angew. Chem., Int. Ed.* **1999**, *38*, 2256.
- (89) Türker, L. *THEOCHEM* **2000**, *531*, 333.
- (90) Bendikov, M.; Duong, H. M.; Starkey, K.; Houk, K. N.; Carter, E. A.; Wudl, F. *J. Am. Chem. Soc.* **2004**, *126*, 7416.
- (91) Raghun, C.; Pati, Y. A.; Ramasesha, S. *Phys. Rev. B* **2002**, *66*, 035116.
- (92) Watson, M. D.; Fechtenkotter, A.; Mullen, K. *Chem. Rev.* **2001**, *101*, 1267.
- (93) See, for example, (a) Bakhshi, A. K.; Liegener, C.-M.; Ladik, J. *Chem. Phys.* **1993**, *173*, 65. (b) Gao, Y.; Liu, C. G.; Jiang, Y. S. *J. Phys. Chem. A* **2002**, *106*, 2592. (c) Cyrański, M. K.; Stepien, B. T.; Krygowski, T. M. *Tetrahedron* **2000**, *56*, 9663.
- (94) Tanaka, K.; Ohzeki, K.; Nankai, S.; Yamabe, T.; Shirakawa, H. *J. Phys. Chem. Solids* **1983**, *44*, 1069. (b) Toussaint, J. M.; Bredas, J. L. *Synth. Met.* **1992**, *46*, 325.
- (95) See, for example, Donohue, J. *The Structures of the Elements*; Wiley: New York, 1974. For the equivalence of CC bonds in graphite, see Freise, E. *J. Nature* **1962**, *193*, 671.
- (96) Yoshizawa, K.; Yumura, T.; Yamabe, T.; Bandow, S. *J. Am. Chem. Soc.* **2000**, *122*, 11871.
- (97) Anno, T.; Coulson, C. A. *Proc. R. Soc. (London)* **1961**, *A264*, 165.
- (98) (a) Baeriswyl, D.; Jeckelmann, E. *Mater. Sci. Forum* **1995**, *191*, 71. (b) Chen, N.; Yang, R. T. *Carbon* **1998**, *36*, 1061.
- (99) Yang, S. Unpublished results.
- (100) (a) Mintmire, J. W.; Dunlap, B. I.; White, C. T. *Phys. Rev. Lett.* **1992**, *68*, 631. (b) Okahara, K.; Tanaka, K.; Aoki, H.; Sato, T.; Yamabe, T. *Chem. Phys. Lett.* **1992**, *219*, 462. (c) Saito, R.; Dresselhaus, G.; Dresselhaus, M. S. *Physical Properties of Carbon Nanotubes*; Imperial College Press: London, 1998; p 35.
- (101) Mintmire, J. W.; White, C. T. *Carbon* **1995**, *33*, 893.
- (102) Chamon, C. *Phys. Rev. B* **2000**, *62*, 2806.
- (103) Kanamitsu, K.; Saito, S. *J. Phys. Soc. Jpn.* **2002**, *71*, 483.
- (104) Sun, G. Y.; Kürti, J.; Kertesz, M.; Baughman, R. H. *J. Phys. Chem. B* **2003**, *107*, 6924. (b) Kürti, J.; Zólyomi, V.; Kertesz, M.; Sun, G.; Baughman, R. H.; Kuzmany, H. *Carbon* **2004**, *42*, 971.
- (105) Strano, M. S.; Dyke, C. A.; Urey, M. L.; Barone, P. W.; Allen, M. J.; Shan, H. W.; Kittrell, C.; Hauge, R. H.; Tour, J. M.; Smalley, R. E. *Science* **2003**, *301*, 1519. (b) Hata, K.; Futaba, D. N.; Mizuno, K.; Namai, T.; Yumura, M.; Iijima, S. *Science* **2004**, *306*, 1362.
- (106) Platt, J. R. *J. Chem. Phys.* **1956**, *25*, 80.
- (107) Labhart, H. *J. Chem. Phys.* **1957**, *27*, 957.
- (108) Buss, V. *Chem. Phys. Lett.* **1973**, *22*, 191.
- (109) Fratev, F.; Enchev, V.; Polansky, O. E.; Bonchev, D. *J. Mol. Struct. (THEOCHEM)* **1982**, *88*, 105.
- (110) Hubbard, J. *Proc. R. Soc. (London)* **1963**, *A276*, 238.
- (111) Lieb, E. H.; Nachtergaele, B. *Int. J. Quantum Chem.* **1996**, *58*, 699.
- (112) Buck, H. *Int. J. Quantum Chem.* **2000**, *77*, 641.
- (113) Čížek, J.; Paldus, J. *J. Chem. Phys.* **1967**, *47*, 3976.
- (114) Yoshizawa, K.; Kato, T.; Yamabe, T. *J. Phys. Chem.* **1996**, *100*, 5697.
- (115) (a) Takahashi, M.; Paldus, J. *Int. J. Quantum Chem.* **1984**, *26*, 349. (b) Takahashi, M.; Paldus, J. *Int. J. Quantum Chem.* **1985**, *28*, 459. (c) Li, X. Z.; Paldus, J. *Int. J. Quantum Chem.* **1996**, *60*, 513.
- (116) Choi, C. H.; Kertesz, M. *J. Chem. Phys.* **1998**, *108*, 6681.
- (117) Wannere, C. S.; Sattelmeyer, K. W.; Schaeffer, H. F., III; Scheyer, P. v. R. *Chem. Int. Ed. Engl.* **2004**, *43*, 4200.
- (118) Eckhardt, H. *J. Chem. Phys.* **1983**, *79*, 2085.
- (119) Yang, S.; Olishevski, P.; Kertesz, M. *Synth. Met.* **2004**, *141*, 171.
- (120) Fokin, A. A.; Jiao, H.; Schleyer, P. v. R. *J. Am. Chem. Soc.* **1998**, *120*, 9364.
- (121) Yoshizawa, K.; Tachibana, M.; Yamabe, T. *Bull. Chem. Soc. Jpn.* **1999**, *72*, 697.
- (122) See, for example, Moroni, L.; Gellini, C.; Salvi, P. R.; Liu, C. J.; Vogel, E. *J. Phys. Chem. A* **2002**, *106*, 6554.
- (123) Jackman, L. M.; Sondheimer, F.; Amiel, Y.; Ben-Efraim, D. A.; Gaoni, Y.; Wolovsky, R.; Bothner-By, A. A. *J. Am. Chem. Soc.* **1962**, *84*, 4307.
- (124) Gaoni, Y.; Sondheimer, F. *Proc. Chem. Soc. London* **1964**, 299.
- (125) Baumann, H.; Oth, J. F. M. *Helv. Chim. Acta* **1995**, *78*, 679.
- (126) Oth, J. F. M. *Pure Appl. Chem.* **1971**, *25*, 573.
- (127) Vogler, H. *J. Mol. Struct.* **1979**, *51*, 289.
- (128) Chiang, C. C.; Paul, I. C. *J. Am. Chem. Soc.* **1972**, *94*, 4741.
- (129) Choi, C. H.; Kertesz, M.; Karpfen, A. *J. Am. Chem. Soc.* **1997**, *119*, 11994.
- (130) Dewar, M. J. S. *The Molecular Orbital Theory of Organic Chemistry*; McGraw-Hill: New York, 1969; p 179.
- (131) Baumann, H.; Bünzli, J. *J. Chem. Soc., Faraday Trans.* **1998**, *94*, 2695.
- (132) Bregman, J.; Hirshfeld, F. L.; Rabinovich, D.; Schmidt, G. M. J. *Acta Crystallogr.* **1965**, *19*, 227.
- (133) Gorter, S.; Keulemans-Rutten, E.; Krever, E.; Romers, C.; Cruickshank, D. W. J. *Acta Crystallogr.* **1995**, *B51*, 1036.
- (134) Oth, J. F. M.; Bünzli, J.; Julien de Zelicourt, Y. *Helv. Chim. Acta* **1974**, *57*, 2276.
- (135) Baumann, H.; Bünzli, J.; Oth, J. F. M. *Helv. Chim. Acta* **1982**, *65*, 582.
- (136) Baumann, H.; Oth, J. F. M. *Helv. Chim. Acta* **1982**, *65*, 1885.
- (137) (a) Van-Catledge, F. A.; Allinger, N. L. *J. Am. Chem. Soc.* **1969**, *91*, 2582. (b) Allinger, N. L. *Adv. Phys. Org. Chem.* **1976**, *13*, 57.
- (138) Dewar, M. J. S.; Haddon, R. C.; Student, P. J. *J. Chem. Soc. Chem. Commun.* **1974**, *14*, 569.
- (139) Kao, J.; Allinger, N. L. *J. Am. Chem. Soc.* **1977**, *99*, 975.
- (140) Haddon, R. C. *Chem. Phys. Lett.* **1980**, *70*, 210.
- (141) Thiel, W. *J. Am. Chem. Soc.* **1981**, *103*, 1420.
- (142) Yoshizawa, K.; Kato, T.; Yamabe, T. *J. Phys. Chem.* **1996**, *100*, 5697. (b) Yoshizawa, K.; Kato, T.; Yamabe, T. *J. Phys. Chem.* **1996**, *100*, 5697.
- (143) (a) Jiao, J.; Schleyer, P. v. R. *Angew. Chem., Int. Ed. Engl.* **1996**, *35*, 2383. (b) Baldrige, K. K.; Siegel, J. S. *Angew. Chem., Int. Ed. Engl.* **1997**, *36*, 745.
- (144) Baumann, H. *J. Am. Chem. Soc.* **1978**, *100*, 7196.
- (145) Jug, K.; Fasold, E. *J. Am. Chem. Soc.* **1987**, *109*, 2263.
- (146) Stevenson, C. D.; Kurth, T. L. *J. Am. Chem. Soc.* **2000**, *122*, 722.
- (147) The discrepancy of MP2 with respect to the more reliable CCSD-(T) energetics has been noted before; see King, R. A.; Crawford, T. D.; Stanton, J. F.; Schaefer, H. F., III. *J. Am. Chem. Soc.* **1999**, *121*, 10788.
- (148) Choi, C. H.; Kertesz, M. Unpublished work.
- (149) See, for example, Parr, R. G. *Quantum Theory of Molecular Electronic Structures*; Benjamin: New York, 1963.
- (150) Kertesz, M. *Phys. Stat. Sol. (b)* **1975**, *69*, K141.
- (151) Perpete, E. A.; Champagne, B. *J. Mol. Struct. (THEOCHEM)* **1999**, *487*, 39.
- (152) Becke, A. D. *J. Chem. Phys.* **1996**, *104*, 1040.
- (153) Becke, A. D. *J. Chem. Phys.* **1993**, *98*, 1372.
- (154) (a) Karpfen, A.; Petkov, J. *Solid State Commun.* **1979**, *29*, 251. (b) Kirtman, B.; Nilsson, W. B.; Palke, W. E. *Solid State Commun.* **1983**, *46*, 791. (c) Villar, H. O.; Dupuis, M.; Watts, J. D.; Hurst, G. V. B.; Clementi, E. *J. Chem. Phys.* **1988**, *88*, 1003. (d) Bredas, J. L.; Toussaint, J. M. *J. Chem. Phys.* **1990**, *92*, 2624. (e) König, G.; Stollhoff, G. *Phys. Rev. Lett.* **1990**, *65*, 1239. (f) Fogarasi, G.; Liu, R.; Pulay, P. *J. Phys. Chem.* **1993**, *97*, 4036. (g) Karpfen, A.; Holler, R. *Solid State Commun.* **1981**, *37*, 179.
- (155) (a) Mintmire, J. W.; White, C. T. *Phys. Rev. B* **1983**, *28*, 3283. (b) Mintmire, J. W.; White, C. T. *Phys. Rev. Lett.* **1983**, *50*, 101. (c) Mintmire, J. W.; White, C. T. *Phys. Rev. B* **1987**, *35*, 4180.
- (156) Ashkenazi, J.; Pickett, W. E.; Wang, C. S.; Krakauer, H.; Klein, B. M. *Bull. Am. Phys. Soc.* **1986**, *31*, 330.
- (157) (a) Hamrin, K.; Johannsson, G.; Gelius, U.; Nordling, C.; Siegbahn, K. *Phys. Scr.* **1970**, *1*, 270. (b) Trickey, S. B.; Ray, A. K.; Worth, J. P. *Phys. Status Solidi B* **1981**, *106*, 613. (c) Boring, M. *Int. J. Quantum Chem.* **1974**, *8*, 451. (d) Zunger, A.; Freeman, A. *J. Phys. Rev. B* **1977**, *16*, 2901.
- (158) Cai, Z. L.; Sendt, K.; Reimers, J. R. *J. Chem. Phys.* **2002**, *117*, 5543.
- (159) Koch, W.; Holthausen, M. C. *A Chemist's Guide to Density Functional Theory*, 2nd ed.; Wiley-VCH: Weinheim, Germany, 2001.
- (160) (a) Springborg, M.; Calais, J.-L.; Goscinski, O.; Eriksson, L. A. *Phys. Rev. B* **1991**, *44*, 12, 713. (b) Springborg, M.; Pohl, A. *J. Phys. Condens. Matter* **1999**, *11*, 7243.
- (161) Barth, U. v.; Hedin, L. *J. Phys. C: Solid State Phys.* **1972**, *5*, 1629.
- (162) Hirata, S.; Torii, H.; Tasumi, M. *J. Chem. Phys.* **1995**, *103*, 8964.
- (163) Salzner, U.; Lagowski, J. B.; Pickup, P. G.; Poirier, R. A. *Synth. Met.* **1998**, *96*, 177.
- (164) Becke, A. D. *J. Chem. Phys.* **1993**, *98*, 5648.
- (165) Yang, S.; Kertesz, M. Unpublished results.

- (166) (a) Suhai, S. *Int. J. Quantum Chem.* **1983**, *23*, 1239. (b) Suhai, S. *Int. J. Quantum Chem.* **1992**, *42*, 193. (c) Sun, J.-Q.; Bartlett, R. J. *J. Chem. Phys.* **1996**, *104*, 8553.
- (167) (a) Suhai, S. *Phys. Rev. B* **1995**, *51*, 16553. (b) Yu, M.; Kalvoda, S.; Dolg, M. *Chem. Phys.* **1997**, *224*, 121.
- (168) Sun, G. Y.; Kürti, J.; Kertesz, M.; Baughman, R. H. *J. Chem. Phys.* **2002**, *117*, 7691.
- (169) A representative review is ref 13a.
- (170) Lee, Y. S.; Kertesz, M. *J. Chem. Phys.* **1988**, *88*, 2609.
- (171) Bredas, J. L. In *Handbook of Conducting Polymers*; Skotheim, T. A., Ed.; Dekker: New York, 1986; Vol. 2, p 859.
- (172) Chance, R. R.; Boudreaux, D. S.; Bredas, J. L.; Silbey, R. In *Handbook of Conducting Polymers*; Skotheim, T. A., Ed.; Dekker: New York, 1986; Vol. 2, p 825.
- (173) See, for example, Bloor, D.; Chance, R. R. *Polydiacetylenes*; NATO ASI E102; Nijhoff: The Hague, 1985.
- (174) (a) Kobelt, v. D.; Paulus, E. F. *Acta Crystallogr. B* **1974**, *30*, 232. (b) Kobayashi, A.; Kobayashi, H.; Tokura, Y.; Kanetake, T.; Koda, T. *J. Chem. Phys.* **1987**, *87*, 4962. (c) Apgar, P. A.; Yee, K. C. *Acta Crystallogr., Sect. B: Struct. Crystallogr. Cryst. Chem.* **1978**, *34*, 957. (d) Hadicke, E.; Mez, E. C.; Krauch, C. H.; Wegner, G.; Kaiser, J. *Angew. Chem.* **1971**, *83*, 253. (e) Bloor, D.; Preston, F. H.; Ando, D. *J. Chem. Phys. Lett.* **1976**, *38*, 33.
- (175) Whangbo, M.-H.; Hoffmann, R.; Woodward, R. B. *Proc. R. Soc.* **1979**, *A366*, 23.
- (176) Tian, B.; Zerbi, G.; Mullen, K. *J. Chem. Phys.* **1991**, *95*, 3198.
- (177) The discussion of polarons and the related bipolarons would be outside the realm of this review. For lead references, see the articles by Campbell, D. K.; Bishop, A. R.; Rice, M. J. and by Chance, R. R.; Boudreaux, D. S.; Bredas, J. L.; Silbey, R. In *Handbook of Conducting Polymers*; Skotheim, T. A., Ed.; Dekker: New York, 1986; Vol. 2.
- (178) Honda, K.; Furukawa, Y.; Furuya, K.; Torii, H.; Tasumi, M. *J. Phys. Chem. A* **2002**, *106*, 3587.
- (179) (a) Bredas, J. L. *J. Chem. Phys.* **1985**, *82*, 3808. (b) Bredas, J. L.; Wudl, F.; Heeger, A. J. *J. Chem. Phys.* **1986**, *85*, 4673. (c) Bredas, J. L. *Synth. Met.* **1987**, *17*, 115.
- (180) Kertesz, M. In *Handbook of Organic Conductive Molecules and Polymers*; Nalwa, H. S., Ed.; John Wiley: New York, 1997; Vol. 4, p 147.
- (181) Mintmire, J. W.; White, C. T.; Elert, M. L. *Synth. Met.* **1986**, *16*, 235.
- (182) Karpfen, A. *J. Phys. C* **1980**, *12*, 5673.
- (183) (a) Parry, D. E. *Chem. Phys. Lett.* **1977**, *46*, 605. (b) Kertesz, M.; Koller, J.; Azman, A. *Chem. Phys.* **1978**, *27*, 273.
- (184) Enkelman, V. In *Polydiacetylenes*; Cantow, H.-J., Ed.; Springer: Berlin, 1984; p 91.
- (185) Tobita, M.; Hirata, S.; Bartlett, R. J. *J. Chem. Phys.* **2001**, *114*, 9130.
- (186) Cottle, A. C.; Lewis, W. F.; Batchelder, D. N. *J. Phys. C: Solid State Phys.* **1978**, *11*, 605.
- (187) Suhai, S. *Phys. Rev. B* **1984**, *29*, 4570.
- (188) Turki, M.; Barisien, T.; Bigot, J.-Y.; Daniel, C. *J. Chem. Phys.* **2000**, *112*, 10526.
- (189) (a) Conwell, E. M. *Synth. Met.* **1996**, *83*, 101. (b) Wohlgenannt, M.; Tandon, K.; Mazumdar, S.; Ramasesha, S.; Vardeny, Z. V. *Nature* **2001**, *409*, 494. (c) Moses, D.; Schmechel, R.; Heeger, A. J. *Synth. Met.* **2003**, *139*, 807. (d) Barford, W.; Bursill, R. J.; Yaron, D. *Phys. Rev. B* **2004**, *69*, 155203.
- (190) See, for example, Kirtman, B.; Champagne, B.; Gu, F. L.; Bishop, D. M. *Int. J. Quantum Chem.* **2002**, *90*, 709.
- (191) Katagiri, H.; Shimoi, Y.; Abe, S. *Chem. Phys.* **2004**, *306*, 191.
- (192) Kertesz, M.; Koller, J.; Azman, A. *Chem. Phys.* **1978**, *27*, 273.
- (193) Tantillo, D. J.; Hoffmann, R.; Houk, K. N.; Warner, P. M.; Brown, E. C.; Henze, D. K. *J. Am. Chem. Soc.* **2004**, *126*, 4256.
- (194) (a) Hoffmann, R.; Hughbanks, T.; Kertesz, M.; Bird, P. H. *J. Am. Chem. Soc.* **1983**, *105*, 4831. (b) Baughman, R. H.; Eckhardt, H.; Kertesz, M. *J. Chem. Phys.* **1987**, *87*, 6687. (c) Baughman, R. H.; Cui, C. *Synth. Met.* **1993**, *55*, 315. (d) Bucknum, M. J.; Hoffmann, R. *J. Am. Chem. Soc.* **1994**, *116*, 11456.
- (195) (a) Martin, R. E.; Diederich, F. *Angew. Chem., Int. Ed.* **1999**, *38*, 1350. (b) Nielsen, M. B.; Diederich, F. *Chem. Rec.* **2002**, *2*, 189.
- (196) For a comprehensive review on polyyne structures, see Szafert, S.; Gladysz, J. A. *Chem. Rev.* **2003**, *103*, 4175.
- (197) Okada, S.; Hayamizu, K.; Matsuda, H.; Masaki, A.; Minami, N.; Nakanishi, H. *Macromolecules* **1994**, *27*, 6259.
- (198) Ikoma, T.; Okada, S.; Nakanishi, H.; Akiyama, K.; Tero-Kubota, S. *Solid State Commun.* **2001**, *117*, 285.
- (199) Ikoma, T.; Okada, S.; Nakanishi, H.; Akiyama, K.; Tero-Kubota, S.; Moberg, K.; Weber, S. *Phys. Rev. B* **2002**, *66*, 014423.
- (200) Ikoma, T.; Okada, S.; Tero-Kubota, S.; Nakanishi, H.; Kato, T.; Hofer, P.; Kamrowski, A.; Akiyama, K. *Appl. Magn. Reson.* **2003**, *23*, 445.
- (201) Calculations on **39** and **40**: Yang, S.; Kertesz, M. To be published.
- (202) Kai, Y.; Yasuoka, N.; Kasai, N.; Akiyama, S.; Nakagawa, M. *Tetrahedron Lett.* **1978**, *19*, 1703.
- (203) Scherf, U. In *Handbook of Conducting Polymers*, 2nd ed.; Skotheim, T. A., Elsenbaumer, R. L., Reynolds, J. R., Eds.; Dekker: New York, 1998; p 363.
- (204) Ukrainskii, I. I. *Theor. Chim. Acta* **1975**, *38*, 179.
- (205) Scherf, U.; Mullen, K. *Macromol. Chem. Macromol. Symp.* **1993**, *69*, 23.
- (206) Huang, J. G. *Acta Chim. Sin.* **2003**, *61*, 694.
- (207) Marsden, J. A.; Palmer, G. J.; Haley, M. M. *Eur. J. Org. Chem.* **2003**, 2355.
- (208) See, for example, Cioslowski, J. *Chem. Phys. Lett.* **1988**, *153*, 446.
- (209) Karpfen, A.; Kertesz, M. *J. Phys. Chem.* **1991**, *95*, 7680.
- (210) Lee, Y. S.; Kertesz, M. *Int. J. Quantum Chem. Quantum Chem. Symp.* **1987**, *21*, 163.
- (211) Wudl, F.; Kobayashi, M.; Heeger, A. J. *J. Org. Chem.* **1984**, *49*, 3382.
- (212) Kürti, J.; Surjan, P. *J. Chem. Phys.* **1990**, *92*, 3247.
- (213) See, for example, Heeger, A. J.; Kivelson, S.; Schrieffer, J. R.; Su, W. P. *Rev. Mod. Phys.* **1988**, *60*, 781.
- (214) (a) Zalis, S.; Kertesz, M. *Synth. Met.* **1992**, *47*, 179. (b) Beljonne, D.; Cornil, J.; Friend, R. H.; Janssens, R. A. J.; Bredas, J. L. *J. Am. Chem. Soc.* **1996**, *118*, 6453.
- (215) Hutchison, G. R.; Zhao, Y. J.; Delley, B.; Freeman, A. J.; Ratner, M. A.; Marks, T. N. *J. Phys. Rev. B* **2003**, *68*, 035204.
- (216) Kwon, O.; McKee, M. L. *J. Phys. Chem.* **2000**, *104*, 7106.
- (217) (a) Hong, S. Y.; Marynick, D. S. *J. Chem. Phys.* **1992**, *96*, 5497. (b) Eckhardt, H.; Shacklette, L. W.; Jen, K. Y.; Elsenbauer, R. L. *J. Chem. Phys.* **1989**, *91*, 1303. (c) Nayak, K.; Marynick, D. S. *Macromolecules* **1990**, *23*, 2237.
- (218) Salzner, U.; Kose, M. E. *J. Phys. Chem. B* **2002**, *106*, 9221.
- (219) Tachibana, M.; Tanaka, S.; Yamashita, Y.; Yoshizawa, K. *J. Phys. Chem. B* **2002**, *106*, 3549.
- (220) (a) Lee, C. H.; Kang, G. W.; Jeon, J. W.; Song, W. J.; Kim, S. Y.; Seoul, C. *Synth. Met.* **2001**, *117*, 75. (b) Chung, T. C.; Kaufman, J. H.; Heeger, A. J.; Wudl, F. *Phys. Rev. B* **1984**, *30*, 702. (c) Zotti, G.; Martina, S.; Wegner, G.; Schluter, A.-D. *Adv. Mater.* **1992**, *4*, 798. (d) Glenis, S.; Benz, M.; LeGoff, E.; Schindler, J. L.; Kannewurf, C. R.; Kanatzidis, M. G. *J. Am. Chem. Soc.* **1993**, *115*, 12519. (e) Groenendaal, L. B.; Jonas, F.; Freitag, D.; Pielartzik, H.; Reynolds, J. R. *Adv. Mater.* **2000**, *12*, 481. (f) Jonas, F.; Schrader, L. *Synth. Met.* **1991**, *41–43*, 831. (g) Meng, H.; Perepichka, D. F.; Wudl, F. *Angew. Chem., Int. Ed.* **2003**, *42*, 658. (h) Kobayashi, M.; Colaneri, N.; Boysel, M.; Wudl, F.; Heeger, A. J. *J. Chem. Phys.* **1985**, *82*, 5717 and 83, 6061. (i) Pomerantz, M.; Chaloner-Gill, B.; Harding, L. O.; Tseng, J. J.; Pomerantz, W. J. *J. Chem. Soc., Chem. Commun.* **1992**, 1672. (j) Meng, H.; Wudl, F. *Macromolecules* **2001**, *34*, 1810. (k) Ikenoue, Y. *Synth. Met.* **1990**, *35*, 263.
- (221) (a) Bakhshi, A. K.; Ago, H.; Yoshizawa, K.; Tanaka, K.; Yamabe, T. *J. Chem. Phys.* **1996**, *104*, 5528. (b) Brocks, G. *J. Phys. Chem.* **1996**, *100*, 17327.
- (222) Hernandez, V.; Castiglioni, C.; Del Zopo, M.; Zerbi, G. *Phys. Rev. B* **1994**, *50*, 9815.
- (223) Kiebooms, R.; Hoogmartens, I.; Adriaensens, P.; Vanderzande, D.; Gelan, J. *Macromolecules* **1995**, *28*, 4961. (b) Zerbi, G.; Magnoni, M. C.; Hoogmartens, I.; Kiebooms, R.; Carleer, R.; Vanderzande, D.; Gelan, J. *Adv. Mater.* **1995**, *7*, 1027.
- (224) (a) Salzner, U. *Curr. Org. Chem.* **2004**, *8*, 569. (b) Ferraris, J. P.; Guerrero, D. J. In *Handbook of Conducting Polymers*, 2nd ed.; Skotheim, T. A., Elsenbaumer, R. L., Reynolds, J. R., Eds.; Dekker: New York, 1998; p 259. (c) Chan, H. S. O.; Ng, S. C. *Prog. Polym. Sci.* **1998**, *23*, 1167.
- (225) See, for example, (a) van Mullekom, H. A. M.; Vekemans, J. A. J. M.; Havinga, E. E.; Meijer, E. W. *Mater. Sci. Eng. Rep.* **2001**, *32*, 1. (b) Salzner, U. *J. Phys. Chem. B* **2002**, *106*, 9214. (c) Berlin, A.; Zotti, G.; Zecchin, S.; Schiavon, G.; Vercelli, B.; Zanelli, A. *Chem. Mater.* **2004**, *16*, 3667. (d) Block, M. A. B.; Khan, A.; Hecht, S. *J. Org. Chem.* **2004**, *69*, 184. (e) Bakhshi, A. K.; Gandhi, G. *Solid State Comm.* **2004**, *129*, 335.
- (226) Jenekhe, J. *Nature* **1986**, *322*, 345.
- (227) Kertesz, M.; Lee, Y. S. *J. Phys. Chem.* **1987**, *91*, 2690.
- (228) Hong, S. Y.; Song, J. M. *Synth. Met.* **1996**, *83*, 141.
- (229) Chen, W. C.; Liu, C. L.; Yen, C. T.; Tsai, F. C.; Tonzola, C. J.; Olson, N.; Jenekhe S. A. *Macromolecules* **2004**, *37*, 5959.
- (230) (a) Bayer, A. G. European Patent 339,340, 1988. Bayer, A. G. *Chem. Abstr.* **1989**, *112*, 159213. (b) Groenendaal, L.; Zotti, G.; Aubert, P.-H.; Waybright, S. M.; Reynolds, J. R. *Adv. Mater.* **2003**, *15*, 855.
- (231) (a) Lorcy, D.; Cava, M. P. *Adv. Mater.* **1992**, *4*, 562. (b) Musmanni, S.; Ferraris, J. P. *J. Chem. Soc. Chem. Commun.* **1993**, 172. (c) Bauerle, P.; Gotz, G.; Segelbacher, U.; Huttenlacher, D.; Mehring, M. *Synth. Met.* **1993**, *55–57*, 4768. (d) Kitamura, C.; Tanaka, S.; Yamashita, Y. *J. Chem. Soc. Chem. Commun.* **1994**, 1585. (e) Lakshminantham, M. V.; Lorcy, D.; Scordilis-Kelley, C.; Wu, X.-L.; Parakka, J. P.; Metzger, R. M.; Cava, J. P. *Adv. Mater.* **1993**, *5*, 723. (f) Metzger, R. M.; Wang,

- P.; Wu, X.-L.; Tormos, G. V.; Lorcy, D.; Shcherbakova, I.; Lakshmikantham, M. V.; Cava, M. P. *Synth. Met.* **1995**, *70*, 1435. (g) Tanaka, S.; Yamashita, Y. *Synth. Met.* **1993**, *55–57*, 1251. (h) Karikomi, M.; Kitamura, C.; Tanaka, S.; Yamashita, Y. *J. Am. Chem. Soc.* **1995**, *117*, 6791. (i) Tanaka, S.; Yamashita, Y. *Synth. Met.* **1995**, *69*, 599. (j) Meng, H.; Tucker, D.; Chaffins, S.; Chen, Y.; Helgeson, R.; Dunn, B.; Wudl, F. *Adv. Mater.* **2003**, *15*, 146. (k) Akoudad, S.; Roncali, J. *Chem. Commun.* **1998**, 2081. (l) Tanaka, S.; Yamashita, Y. *Synth. Met.* **1997**, *84*, 229.
- (232) Kürti, J.; Surjan, P. R.; Kertesz, M.; Frapper, G. *Synth. Met.* **1993**, *55–57*, 4338.
- (233) Lee, Y.-S.; Kertesz, M.; Elsenbaumer, R. L. *Chem. Mater.* **1990**, *2*, 526. (b) Hong, S. Y.; Kim, S. C. *Bull. Korean Chem. Soc.* **2003**, *24*, 1649.
- (234) (a) Baigent, D. R.; Hamer, P. J.; Friend, R. H.; Moratti, S. C.; Holmes, A. B. *Synth. Met.* **1995**, *71*, 2175. (b) Hagan, A. J.; Moratti, S. C.; Sage, I. C. *Synth. Met.* **2001**, *119*, 147. (c) Sonmez, G.; Meng, H.; Wudl, F. *Chem. Mater.* **2003**, *15*, 4923. (d) Lee, K.; Sotzing, G. A. *Macromolecules* **2001**, *34*, 5746. (e) Kim, I. T.; Elsenbaumer, R. L. *Macromolecules* **2000**, *33*, 6407.

CR990357P